THE JOURNAL OF BIOLOGICAL CHEMISTRY VOL. 286, NO. 51, pp. 43793–43808, December 23, 2011

SUMOylation and SUMO-interacting Motif (SIM) of Metastasis Tumor Antigen 1 (MTA1) Synergistically Regulate Its Transcriptional Repressor Function*[S]

Received for publication, June 1, 2011, and in revised form, September 28, 2011 Published, JBC Papers in Press, September 30, 2011, DOI 10.1074/jbc.M111.267237

Lin Cong[‡], Suresh B. Pakala[‡], Kazufumi Ohshiro[‡], Da-Qiang Li[‡], and Rakesh Kumar[‡§1]

From the [‡]Department of Biochemistry and Molecular Biology, School of Medicine and Health Sciences, George Washington University, Washington, D. C. 20037 and the [§]Cancer Research Program, Rajiv Gandhi Centre for Biotechnology, Thiruvananthapuram 695014, India

Background: The mechanism by which MTA1 modulates gene repression remains largely unknown.
Results: SUMOylated Lys-509 in conjunction with SIM is involved in MTA1-mediated repression of its target gene *PS2*, probably by recruiting HDAC2.
Conclusion: SUMOylation at Lys-509 together with SIM synergistically regulates MTA1-mediated repression.
Significance: This is a new regulatory mechanism by which MTA1 represses target gene expression.

Metastasis tumor antigen 1 (MTA1), a component of the Mi-2·nucleosome remodeling and deacetylase complex, plays a crucial role in gene transcription, but the mechanism involved remains largely unknown. Here, we report that MTA1 is a substrate for small ubiquitin-related modifier 2/3 (SUMO2/3) *in vivo*. Protein inhibitor of activated STAT (PIAS) proteins enhance SUMOylation of MTA1 and may participate in paralog-selective SUMOylation, whereas sentrin/SUMO-specific protease 1 (SENP1) and 2 may act as deSUMOylation enzymes for MTA1. Moreover, MTA1 contains a functional SUMO-interacting motif (SIM) at its C terminus, and SIM is required for the efficient SUMOylation of MTA1. SUMO conjugation on Lys-509, which is located within the SUMO consensus site, together with SIM synergistically regulates the co-repressor activity of MTA1 on *PS2* transcription, probably by recruiting HDAC2 onto the *PS2* promoter. Interestingly, MTA1 may up-regulate the expression of *SUMO2* via interaction with RNA polymerase II and SP1 at the *SUMO2* promoter. These findings not only provide novel mechanistic insights into the regulation of the transcriptional repressor function of MTA1 by SUMOylation and SIM but also uncover a potential function of MTA1 in modulating the SUMOylation pathway.

Posttranslational modification by the small ubiquitin-related modifier (SUMO)[2] plays important roles in the regulation of diverse cellular processes, including protein stabilization, subcellular localization and gene transcription (1–3). In mammals, three major SUMO isoforms, SUMO1–3, have been identified. SUMO2 and SUMO3 are almost identical, as they share about 97% amino acid sequence identity and collectively are referred to as SUMO2/3 in most cases, whereas SUMO1 exhibits ~50% amino acid sequence identity with SUMO2 and SUMO3.

SUMO is attached covalently to ϵ-lysine embedded in the φK*X*E motif (φ represents hydrophobic amino acid, and *X* stands for any amino acid) within the target protein in an enzymatic cascade similar to ubiquitination. SUMO conjugation requires one SUMO-activating enzyme, E1 (Aos1/Uba2); a single conjugating enzyme, E2 (UBC9); and in some cases, additional E3 ligases (4). Like many cellular processes, SUMOylation is a highly dynamic process and can be reversed by a family of sentrin/SUMO-specific proteases (SENPs) (5). SUMO can interact noncovalently with protein through the SUMO-interacting motif (SIM) in the target as well. To date, the best featured class of SIM consists of a hydrophobic core ((V/I)*X*(V/I)(V/I)) flanked by acidic amino acids, which together may contribute to SUMO binding affinity, orientation, and paralog selection (6). Some SUMO substrates also contain one or more functional SIMs (7, 8), but how SUMOylation and SIM act together in modulating gene transcription is largely unknown.

Metastasis tumor antigen 1 (MTA1), a component of the Mi-2·nucleosome remodeling and deacetylase (NuRD) complex, is widely up-regulated in human cancers and plays a crucial role in tumorigenesis and tumor metastasis (9). It has been established that MTA1 modulates gene transcription by interacting with a co-repressor (*e.g.* HDAC2) or a co-activator (*e.g.* MiCoA), depending on the promoter context (10–12). It is of interest to determine how MTA1 coordinates this association with different co-regulators. Posttranslational modification could be one useful way. Recent studies suggest that the activity of MTA1 can be regulated dynamically by ubiquitination and acetylation. Reduced MTA1 ubiquitination contributes to its stability and then exerts its function in DNA damage repair (13). Acetylated MTA1 is required for the activation of the Ras-Raf pathway (14). However, whether MTA1 could be SUMO-

* This work was supported, in whole or in part, by National Institutes of Health Grants CA98823 and CA98823-S1 (to R. K.).
[S] The on-line version of this article (available at http://www.jbc.org) contains supplemental Figs. S1–S5.
[1] To whom correspondence should be addressed. E-mail: bcmrxk@gwumc.edu.
[2] The abbreviations used are: SUMO, small ubiquitin-related modifier; SIM, SUMO-interacting motif; MTA1, metastasis tumor antigen 1; PIAS, protein inhibitor of activated STAT; SENP, sentrin/SUMO-specific protease; Ni-NTA, nickel-nitrilotriacetic acid; NuRD, nucleosome remodeling and deacetylase; ERE, estrogen-responsive element; AAA, triple mutant I711A/V712A/I713A; MEF, mouse embryonic fibroblast; Pol II, RNA polymerase II.

ylated and how its functions are influenced by SUMO remain unknown.

Here, we report that MTA1 is a SUMO2/3 substrate *in vivo* and define one functional SIM in its C terminus. The SIM of MTA1 is required for efficient SUMO conjugation of MTA1 but not paralog-selective SUMOylation, which may be regulated by protein inhibitor of activated STAT (PIAS) proteins. Moreover, SUMOylation of MTA1 at Lys-509 within the SUMO consensus site together with SIM may synergistically regulate MTA1-mediated repression of *PS2* by recruiting HDAC2 onto the *PS2* promoter. In addition, MTA1 up-regulates the expression of *SUMO2*. These findings not only suggest a synergistic regulatory mechanism of SUMO modification and SIM in MTA1-mediated gene transcription but also reveal a possible function of MTA1 in regulating the SUMOylation pathway.

EXPERIMENTAL PROCEDURES

DNA Constructs—pCMV-Myc-MTA1, full-length pcDNA-T7-MTA1 and its fragments (residues 1–164, 1–226, 1–441, 227–388, 442–715, and 542–715), and the Gal4–3×ERE reporter gene have been described previously (10, 15). pcDNA-T7-MTA1 fragments (residues 442–710, 542–710, 442–541, 542–636, 637–715, and 637–710) were generated by cloning MTA1 fragments into the pcDNA3.1/HisA vector (Invitrogen). Plasmids encoding EGFP-tagged human SUMO1 and SUMO2 and T7-tagged PIAS family proteins (1, 3, and y) were a kind gift from Mary Dasso (National Institutes of Health). Conjugatable forms of GST-tagged or His-tagged SUMO1 or SUMO2 were obtained by cloning the cDNAs of SUMO1 and SUMO2 from EGFP·SUMO1 and EGFP·SUMO2 in-frame with the GST tag in pGEX-4T-1 vector (GE Healthcare) or the His tag in pcDNA3.1/HisC vector (Invitrogen). The fragments containing His-SUMO1 or His-SUMO2 were amplified by PCR and inserted into pCMV-HA (Clontech, Palo Alto, CA) to generate the HA-His-tagged SUMO1 or SUMO2 expression vector. GST·SUMO1GA and GST·SUMO2GA were obtained by mutating the last glycine residue (the 97th glycine residue in SUMO1, the 93rd glycine residue in SUMO2) to an alanine residue with a QuikChange site-directed mutagenesis kit (Stratagene, La Jolla). pcDNA-FLAG-PIAS expression vectors (1, 3, and y) were a kind gift from Jorma J. Palvimo (Biomedicum Helsinki, Institute of Biomedicine, Helsinki, Finland). pcDNA-FLAG-SENP expression plasmids (the wild type 1, 2, 3, and their inactive mutants, SENP1-C603S, SENP2-C547S, and SENP3-C532A) were kindly provided by Andrew D. Sharrocks (University of Manchester, Manchester, United Kingdom). pGEX-4T-UBC9 and pcDNA-FLAG-UBC9 plasmids were obtained from Frank J. Rauscher III (Wistar Institute, Philadelphia). The *PS2* reporter expression plasmid was kindly provided by David J. Shapiro (University of Illinois). Gal4-MTA1 was kindly provided by Weidong Wang (National Institutes of Health). The Gal4-MTA1-K509R mutant, pcDNA-T7-MTA1 mutants, and pCMV-Myc-MTA1 mutants were obtained by using a site-directed mutagenesis kit as described above. All plasmids were confirmed by DNA sequencing analysis.

Cell Culture and Reagents—Human breast cancer MCF-7 cells and monkey kidney COS-1 cells were maintained in Dulbecco's modified Eagle's medium/Ham's F-12 50/50 mix (Cellgro, Manassas, VA) supplemented with 10% fetal bovine serum (Atlanta Biologicals, Lawrenceville, GA). All cells were incubated at 37 °C in a humidified environment with 5% CO_2. For 17β-estradiol treatment, regular medium was replaced by improved minimum essential medium (IMEM) containing 5% charcoal-dextran-stripped fetal bovine serum (Atlanta Biologicals).

Mouse anti-SUMO1, mouse anti-MTA1, and rabbit anti-HDAC2 antibodies were purchased from Santa Cruz Biotechnology (Santa Cruz, CA). Rabbit anti-SUMO2/3 antibody was purchased from Abcam (Cambridge, MA). Mouse anti-Myc antibody was purchased from NeoMarkers (Fremont, CA). Mouse anti-FLAG (M2) antibody was purchased from Sigma. Rabbit anti-MTA1, anti-MTA2, and anti-T7 antibodies were purchased from Bethyl Laboratories (Montgomery, TX). Mouse anti-T7 antibody was purchased from Novagen (Milwaukee, WI). Mouse anti-HA and rabbit anti-UBC9 antibodies were purchased from Cell Signaling Technology (Danvers, MA). Nonidet P-40, 17β-estradiol, Tris(2-carboxyethyl)phosphine, deSUMOylation inhibitor *N*-ethylmaleimide, and iodoacetamide were purchased from Sigma. Protease mixture inhibitor was purchased from Roche Applied Science.

Co-immunoprecipitation—Cells were lysed directly in Nonidet P-40 lysis buffer (150 mM NaCl, 50 mM HEPES (pH 7.5), 1% Nonidet P-40, and 1 mM dithiothreitol (DTT)) containing 20 mM *N*-ethylmaleimide and 10 mM iodoacetamide to minimize deSUMOylation plus protease inhibitor mixture. Cell lysates were incubated with the indicated antibodies at 4 °C overnight. The immunoprecipitates were collected on protein A/G-Sepharose beads (Santa Cruz Biotechnology). The beads were washed with Nonidet P-40 lysis buffer three times and boiled in 2× SDS sample buffer. The bound proteins were separated by SDS-PAGE and subjected to Western blotting.

Denaturing immunoprecipitation was performed as described previously (16). Briefly, cells were washed with ice-cold PBS and lysed with SDS lysis buffer (4% SDS, 10 mM DTT, 300 mM NaCl, and 10 mM HEPES (pH 7.5)) supplemented with 20 mM *N*-ethylmaleimide, 10 mM iodoacetamide, and protease inhibitor mixture at 100 °C for 5 min. The lysates were diluted 10-fold with dilution buffer (1.7% Thesit, 150 mM NaCl, and 50 mM HEPES (pH 7.5)) and then incubated with the indicated primary antibodies at 4 °C overnight. The immunoprecipitates were collected on protein A/G-Sepharose beads followed by washing with washing buffer (0.5% Thesit, 150 mM NaCl, and 50 mM HEPES (pH 7.5)) four times and boiling in 2× SDS sample buffer. The bound proteins were separated by SDS-PAGE and subjected to Western blotting.

In Vitro and in Vivo SUMOylation and deSUMOylation Assays—For the *in vitro* SUMOylation assay, T7-tagged MTA1-WT and its mutants were generated by *in vitro* transcription/translation in the presence of ^{35}S-labeled methionine using the TnT T7 Quick Coupled Transcription/Translation System (Promega, Madison, WI). Unless otherwise noted, *in vitro* SUMOylation reactions were performed at 37 °C for 1.5 h with the mixture including 75 ng of Aos1/Uba2 (LAE Biotech International, Rockville, MD), 1.5 μg of GST-UBC9, 1 μg of SUMO1 or SUMO2, 2 mM ATP, and 1 μl of ^{35}S-labeled and *in*

vitro translated T7-tagged MTA1 or its mutants in a total volume of 20 μl. Reaction buffer was composed of 20 mM Tris-HCl (pH 7.5), 100 mM NaCl, 5 mM $MgCl_2$, 0.4 mM DTT, and 0.05% Tween 20. For the E3 ligase assay, equal amounts of *in vitro* translated, unlabeled, T7-tagged PIAS proteins were added to the reactions containing 0.03 μg of GST-UBC9. For the *in vitro* deSUMOylation assay, SUMO2-modified MTA1 was prepared as described above and incubated with equal amounts of *in vitro* translated, unlabeled, FLAG-tagged SENP-WT or their inactive mutants at 37 °C for 1.5 h. The reaction products were analyzed by SDS-PAGE followed by direct autoradiography.

For the *in vivo* SUMOylation and deSUMOylation assays, COS-1 or MCF-7 cells were co-transfected with the indicated expression vectors. Cell lysate preparation and nickel-nitrilotriacetic acid (Ni-NTA; Qiagen, Valencia, CA) pulldown were performed as described previously (17). The proteins were analyzed by Western blotting with anti-Myc mouse antibody.

GST Pulldown Assay—^{35}S-Labeled, *in vitro* translated proteins or MCF-7 cell lysates were incubated with GST control or GST fusion proteins and glutathione-Sepharose beads (GE Healthcare) at 4 °C overnight in binding buffer (25 mM Tris-HCl (pH 8.0), 3 mM KCl, 140 mM NaCl, 0.1% Nonidet P-40, and 1 mM DTT) supplemented with protease inhibitor mixture. After washing, bound proteins were eluted with 2× SDS sample buffer and analyzed by Western blotting followed by direct autoradiography or with the indicated antibodies.

Immunofluorescence Staining—MCF-7 cells were cultured on coverslips in 6-well plates. The cells were washed briefly with ice-cold PBS, fixed with 4% paraformaldehyde, permeabilized in 0.1% Triton X-100 for 10 min, and then washed with cold PBS three times. The cells were incubated with the indicated primary antibodies for 1 h followed by incubation with Alexa Fluor secondary antibodies (Molecular Probes, Eugene, OR).

Luciferase Assay—MCF-7 cells (3×10^5) were plated in 6-well plates with IMEM supplemented with 5% charcoal-dextran-stripped fetal bovine serum 24 h before transfection. The cells were co-transfected with 200 ng of reporter plasmid, the indicated expression constructs, and 10 ng of pSV-β-galactosidase control vector encoding β-galactosidase used for internal control using FuGENE6 (Roche Applied Science). Twenty-four hours after transfection, the cells were induced with 10 nM 17β-estradiol and then collected and lysed after another 24 h and assayed for luciferase activity following the manufacturer's instructions (Promega). Luciferase activity was normalized to the activity of the internal standard, β-galactosidase. Each experiment was repeated three times.

Chromatin Immunoprecipitation—Total 10^6 MCF-7 cells were cross-linked by 1% formaldehyde solution. The chromatin immunoprecipitation (ChIP) assay was performed as described previously (10). After immunoprecipitation with the corresponding antibodies, the eluted DNA was amplified by PCR. For human *SUMO2* promoter, the following primers used were: R1, 5′- AGGGACAAAAGGAAATAATAAAG-3′ (sense) and 5′- ATATTCATGTATTCATTCAACGAG-3′ (antisense); R2, 5′-GAGAGTGTTGATCTGAACTAGATG-3′ (sense) and 5′-ATCTTGTCTATTCCACCTTCTTAC-3′ (antisense); and R3, 5′-CATATTGCAGTATCTTTGTGTTTT-3′ (sense) and 5′-AAACCCAGTGTCTCTACTAAAAAT-3′ (antisense).

siRNA Transfection—siRNA targeting MTA1 or UBC9 and negative control siRNA were purchased from Dharmacon (Lafayette, CO). MCF-7 cells were seeded at 40% density 1 day before transfection, and siRNA transfection was performed with Oligofectamine reagent (Invitrogen) according to the manufacturer's instructions. Cells were harvested 48–72 h after transfection, and cell lysates or total RNA was prepared.

Quantitative RT-PCR—Quantitative RT-PCR was performed by using iQ™ SYBR Green Supermix (Bio-Rad Laboratories) on a CFX96 real-time PCR detection system (Bio-Rad). The primers used for mRNA expression levels were as follows: for human *PS2*, 5′-CACCATGGAGAACAAGGTGA-3′(sense) and 5′-TGACACCAGGAAAACCACAA-3′ (antisense); for human *UBC9*, 5′-CAGGAGAGGAAAGCATGGAG-3′ (sense) and 5′-TCGGGTGAAATAATGGTGGT-3′ (antisense); for human *SUMO2*, 5′-GCAGACGGGAGGTGTCTACT-3′(sense) and 5′-AGTCAGGATGTGGTGGAACC-3′ (antisense); for human and mouse *MTA1*, 5′-TGCTCAACGGGAAGTCCTAC-3′ (sense) and 5′-GTTTCCGAGGATGAGAGCAG-3′ (antisense); for mouse *SUMO2*, 5′-CAGCCAATCAACGAAACAGA-3′ (sense) and 5′-ATGTGGTGGGACCAAATTGT-3′ (antisense); for human *β-actin*, 5′-GGACTTCGAGCAAGAGATGG-3′ (sense) and 5′-AGCACTGTGTTGGCGTACAG-3′ (antisense); and for mouse *β-actin*, 5′-GTCGTACCACAGGCATTGTGATGG-3′ (sense) and 5′-GCAATGCCTGGGTACATGGTGG-3′ (antisense). The primers of *PS2* used for ChIP were: 5′-TGGGCTTCATGAGCTCC-3′ (sense) and 5′-TACTCATATCTGAGAGGCCCT-3′ (antisense).

Statistical Analysis—A publicly available breast cancer data set, GSE 3494-HGU133A was used to analyze the correlation between *MTA1* and *SUMO2*. The data set consists of samples from 251 freshly frozen primary tumors from breast cancer patients in Uppsala County, Sweden. The probes used to detect the transcript levels of *MTA1* were 202247_s_at and 211783_s_at, and those used for *SUMO2* levels were 208739_x_at, 215452_x_at, 208738_x_at, and 213881_x_at. The intensity values for each of the probes were preprocessed and summarized using GeneSpring GX 11.0. The z-score for each probe in each sample was then calculated and averaged for further analysis. Pearson's correlation test was used to analyze the correlation between *MTA1* and *SUMO2* in the chosen data set by using the mean z-score.

RESULTS

MTA1 Can Be SUMOylated—While searching for the potential SUMO consensus site in MTA1 (SUMOsp2.0), we found that human MTA1 contains only one highly conserved SUMO consensus site across species, IKAE (residues 508–511), which is located outside all functional domains (Fig. 1*A*). We first used a reconstituted *in vitro* SUMO modification system to examine whether MTA1 could be SUMOylated. To this aim, ^{35}S-labeled, *in vitro* translated, full-length MTA1 was incubated with recombinant Aos1/Uba2 (E1), GST-UBC9 (E2), SUMO1, or SUMO2 in the presence of ATP. In the control reaction without the E1 enzyme, a unique, major band of MTA1, which migrated

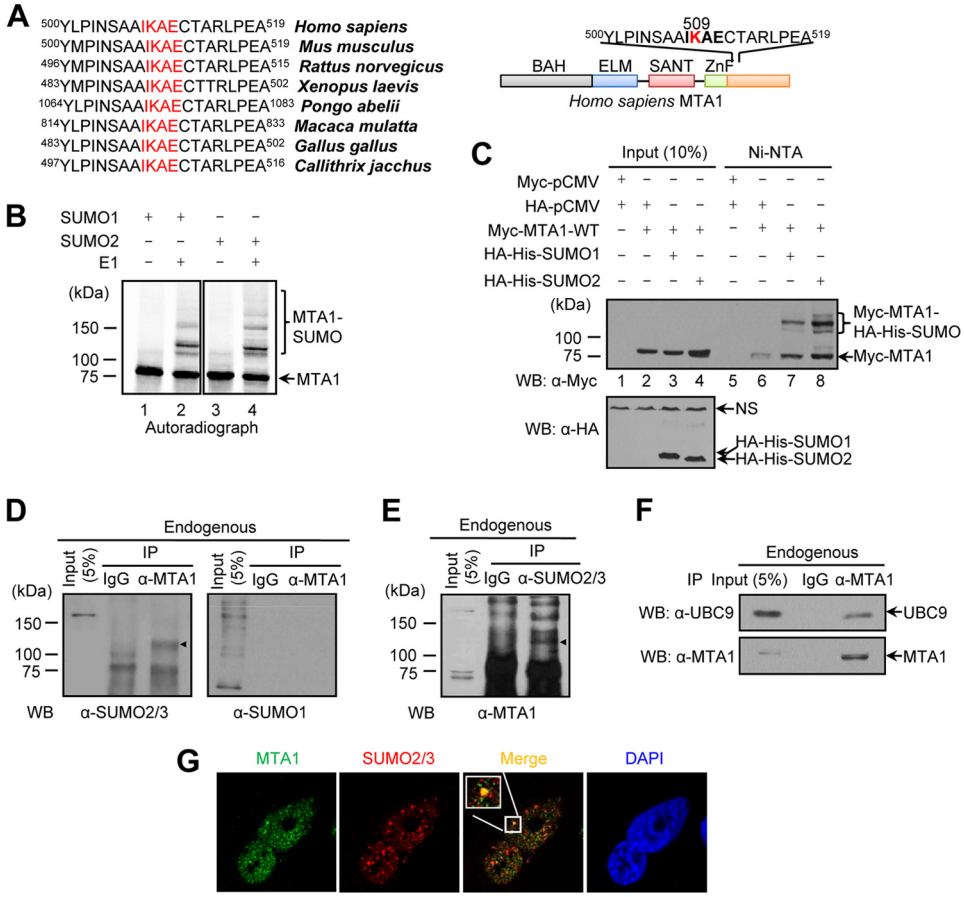

FIGURE 1. **MTA1 undergoes SUMOylation.** *A*, *left*, the SUMO consensus site (IKAE) in MTA1, labeled in *red*, is conserved across species (*left*). *Right*, schematic drawing of the position of the SUMO consensus site (IKAE, *bold*) in human MTA1; the lysine residue embedded in this site is labeled in *red*. *B*, MTA1 is modified by SUMO proteins *in vitro*. ^{35}S-Labeled, *in vitro* translated MTA1-WT was incubated with either SUMO1 or SUMO2. The reaction products were resolved by SDS-PAGE and detected by autoradiography. *C*, MTA1 is modified by SUMO proteins *in vivo*. COS-1 cells were co-transfected with the indicated expression vectors. Forty-eight hours after transfection, a fraction of the cells was lysed in denaturing guanidine-HCl lysis buffer, and the SUMOylated proteins were recovered on Ni-NTA beads and subjected to Western blotting (*WB*) with anti-Myc mouse antibody. Another fraction of the cells was lysed in Nonidet P-40 lysis buffer and subjected to Western blotting with the indicated antibodies for analysis of protein expression. *NS*, nonspecific. *D*, endogenous MTA1 is modified by SUMO2/3 but not SUMO1. MCF-7 cells were harvested under denaturing conditions as described under "Experimental Procedures" and immunoprecipitated with anti-MTA1 rabbit antibody. The immunoprecipitates (*IP*) were resolved by SDS-PAGE and immunoblotted with anti-SUMO2/3 rabbit antibody (*left panel*). The same blot was stripped and reprobed with anti-SUMO1 mouse antibody (*right panel*). *E*, MCF-7 cells were harvested under denaturing conditions prior to immunoprecipitation with anti-SUMO2/3 rabbit antibody followed by immunoblotting with anti-MTA1 rabbit antibody. In *D* and *E*, SUMOylated MTA1 is indicated by an *arrowhead*. *F*, endogenous MTA1 interacts with UBC9. The MCF-7 cell lysates were immunoprecipitated with anti-MTA1 rabbit antibody followed by Western blotting with anti-UBC9 or anti-MTA1 rabbit antibody. *G*, endogenous MTA1 co-localizes with SUMO2/3. MCF-7 cells were fixed and stained with anti-MTA1 mouse antibody (*green*) and anti-SUMO2/3 rabbit antibody (*red*). DNA was stained with DAPI. The images were taken by confocal microscopy.

to 75 kDa, was detected (Fig. 1*B*, *lanes 1* and *3*). In contrast, the addition of the E1 enzyme to the reaction containing SUMO1 or SUMO2 resulted in the formation of equal poly-SUMO chains (Fig. 1*B*, *lanes 2* and *4*). These results suggest that MTA1 can be modified equally by either SUMO1 or SUMO2 *in vitro*.

To examine whether SUMO paralogs could modify MTA1 *in vivo*, Myc-tagged MTA1 was co-expressed with HA-His-tagged SUMO1 or SUMO2 in COS-1 cells. After affinity purification, multiple shifted bands, representing SUMOylated MTA1, were detected around 120–130 kDa in the samples overexpressing HA-His-tagged SUMO1 or SUMO2. The SUMO2-modified MTA1 showed more retention on Ni-NTA beads than SUMO1-modified MTA1 (Fig. 1*C*, *lane 7 versus 8*). In addition, we observed a band at 75 kDa (Fig. 1*C*, *lanes 6–8*) corresponding to unmodified Myc-tagged MTA1 (Fig. 1*C*, *lanes 2–4*), most likely retained on Ni-NTA beads via the zinc finger motif as described previously for HIC1 (18).

Next, we tested SUMOylation of endogenous MTA1 by performing a denaturing immunoprecipitation using MCF-7 cell extracts. After immunoprecipitation with anti-MTA1 rabbit antibody, one dispersed shifted band at about 110–120 kDa was detected when blotted with anti-SUMO2/3 rabbit antibody (Fig. 1*D*, *left panel*) but not with anti-SUMO1 mouse antibody (Fig. 1*D*, *right panel*). In addition, one band around 120 kDa was also detected by performing a reciprocal denaturing immunoprecipitation with anti-SUMO2/3 rabbit antibody followed by Western blotting with anti-MTA1 rabbit antibody (Fig. 1*E*). The different number of bands around 120 kDa, which were observed in the denaturing immunoprecipitation and Ni-NTA pulldown assay, probably resulted from the antibodies we used, because the result from the *in vitro* SUMOylation assay correlated with that seen in the Ni-NTA pulldown assay. Moreover, we found that endogenous MTA1 interacted with UBC9 *in vivo* when co-immunoprecipitation was performed (Fig. 1*F*). Fur-

thermore, endogenous MTA1 and SUMO2/3 showed a clear co-localization in MCF-7 cells (Fig. 1*G*). Taken together, all of the above results confirm that MTA1 is a potent SUMO substrate and is modified preferentially by SUMO2/3 *in vivo*. Interestingly, MTA2, another member of the MTA family that contains the same SUMO consensus site (IKAE) as MTA1, can also be modified by SUMO2/3 but not by SUMO1 *in vivo* (supplemental Fig. S1).

Lys-509 Is the Major SUMO Acceptor in MTA1—To address the potential target site for SUMO modification, Lys-509, which is located in the highly conserved SUMO consensus site in MTA1 (Fig. 1*A*, *right panel*), was mutated to an arginine residue. The wild type (WT) and the K509R mutant of ^{35}S-labeled MTA1 were generated and subjected to an *in vitro* SUMOylation assay. With MTA1-WT, two close, slower migrating bands around 110–120 kDa were detected (Fig. 2*A*, *lanes 2* and *5*). In contrast, the upper band (Fig. 2*A*, *arrowheads*) significantly decreased with the K509R mutant (Fig. 2*A*, *left panel*, *lane 2 versus 3*) and was absent when using a low concentration of GST-UBC9 (Fig. 2*A*, *right panel*, *lane 5 versus 6*), but the lower band remained. To further confirm these findings, COS-1 cells were co-transfected with the Myc-tagged MTA1-WT or MTA1-K509R mutant and HA-His-tagged SUMO2 constructs. After Ni-NTA affinity purification, only one strong band (Fig. 2*B*, *arrowhead*) was missing in the K509R mutant compared with that in the WT (*lane 3 versus 4*). These results indicate that Lys-509 is the major SUMO acceptor site and both consensus and non-consensus sites are involved in the SUMOylation of MTA1.

Besides Lys-509, there are another two lysine residues (Lys-41 and Lys-350) located in two inverted SUMO consensus sites (^{39}EAKV^{42} and ^{348}ESKL^{351}) within MTA1. As the mutation of Lys-509 to arginine did not completely abolish SUMOylation of MTA1, we assumed that Lys-41 and Lys-350 might function as SUMO acceptor sites as well. However, we could not detect any difference between the K509R mutant and the mutants harboring K41R or K350R along with K509R when performing the *in vitro* SUMOylation assay (Fig. 2*C*, *lanes 7* and *8 versus 3*). Similar results were obtained when we attempted to identify other potential SUMOylation sites (Fig. 2*C*, *lanes 4–6 versus 3*). Based on these results, we focused on investigating the function of SUMO conjugation on Lys-509 in the subsequent study.

PIAS Family Proteins Enhance SUMOylation of MTA1—Although MTA1 can be SUMOylated in the reactions without E3 ligase (Fig. 1*B*), we could not exclude the possibility that an E3 ligase might be required for SUMOylation of MTA1. PIAS proteins and RanBP2 are well known E3 ligases in the SUMO conjugation pathway (4, 19). Because MTA1 is located primarily in the nucleus (Fig. 1*G*), we hypothesized that PIAS proteins, which are also located mainly in the nucleus, might function as E3 ligases for the SUMO modification of MTA1. To test this hypothesis, *in vitro* translated PIAS proteins were added to the SUMOylation reactions in the presence of limited recombinant GST-UBC9 (0.03 μg in 20 μl). As shown in Fig. 3*A*, the addition of PIAS3 significantly enhanced the formation of SUMO2-conjugated MTA1 (Fig. 3*A*, *lane 3*). In contrast, PIAS1 and PIASy have a moderate effect on the SUMOylation of MTA1 (Fig. 3*A*, *lanes 2* and *4*). To confirm these results *in vivo*, COS-1 cells were co-transfected with Myc-tagged MTA1 and limited HA-His-tagged SUMO2 (0.2 μg) expression vectors, alone or together with FLAG-tagged PIAS1, PIAS3, or PIASy constructs. Consistent with the above results, we found that all of the indicated PIAS proteins stimulated the modification by SUMO2 and that PIAS3 (Fig. 3*B*, *lane 4*) showed more conju-

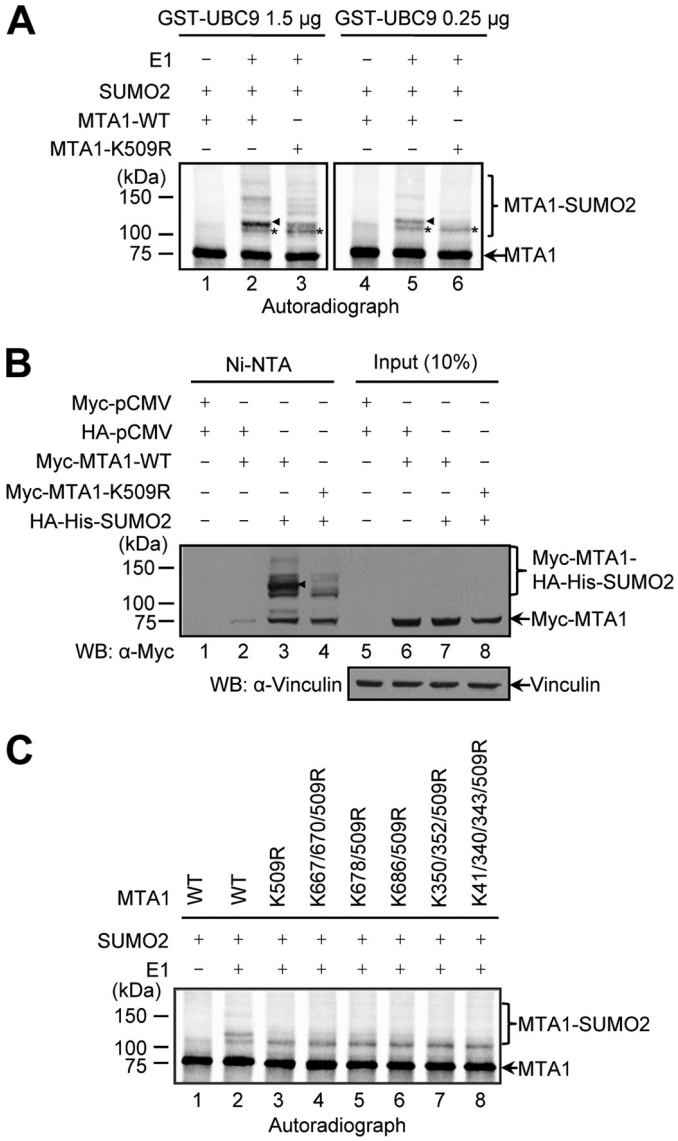

FIGURE 2. **Lys-509 is the major SUMO acceptor in MTA1.** *A*, Lys-509 is identified as a major SUMO acceptor *in vitro*. ^{35}S-Labeled, *in vitro* translated MTA1-WT or MTA1-K509R mutant was incubated in SUMOylation reactions containing SUMO2 and 1.5 μg (*left panel*) or 0.25 μg (*right panel*) of GST-UBC9. The reaction products were resolved by SDS-PAGE and detected by autoradiography. The bands representing SUMO2 conjugation on Lys-509 and the lysine residue within the non-consensus site are indicated by an *arrowhead* and an *asterisk*, respectively. *B*, Lys-509 is identified as a major SUMO acceptor *in vivo*. COS-1 cells were co-transfected with the indicated expression vectors. HA-His-SUMO2 conjugates were purified by Ni-NTA beads and analyzed by Western blotting (*WB*) with anti-Myc mouse antibody. Expression levels of Myc-tagged MTA1 and vinculin are shown as *input*. The band representing SUMO2 conjugation on Lys-509 is indicated by an *arrowhead*. *C*, identification of potential SUMOylation sites other than Lys-509 in MTA1 *in vitro*. MTA1-WT or its indicated mutants were generated by ^{35}S-labeled *in vitro* translation and incubated in SUMOylation reactions containing SUMO2 and 0.25 μg of GST-UBC9. The reaction products were resolved by SDS-PAGE and detected by autoradiography.

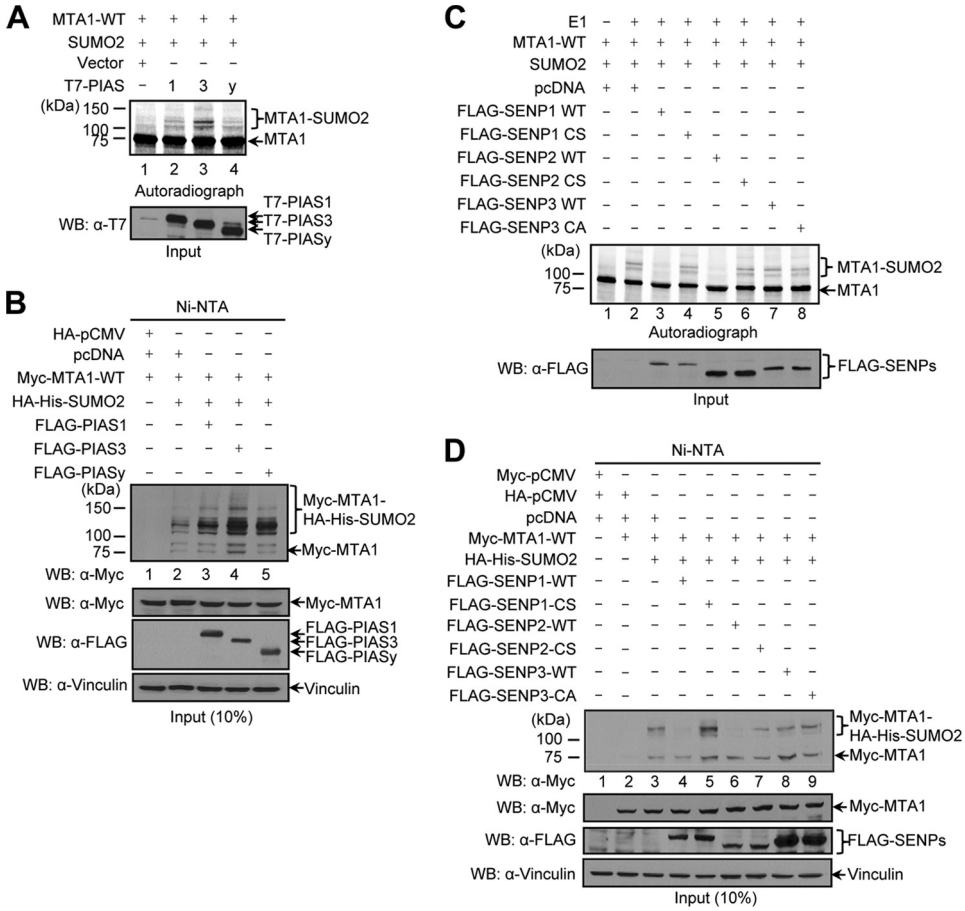

FIGURE 3. **PIAS proteins and SENP1/2 regulate SUMOylation of MTA1.** *A*, PIAS proteins enhance SUMOylation of MTA1 *in vitro*. The same amounts of unlabeled, *in vitro* translated PIAS1, PIAS3, or PIASy were incubated with ^{35}S-labeled, *in vitro* translated MTA1 in SUMOylation reactions containing SUMO2 and a limited concentration of GST-UBC9 (0.03 μg in 20 μl volume). The reaction products were resolved by SDS-PAGE and detected by autoradiography. Anti-T7 Western blotting (*WB*) showed the amounts of PIAS proteins used in this assay. *B*, PIAS proteins enhance SUMOylation of MTA1 *in vivo*. COS-1 cells were co-transfected with the indicated expression vectors. HA-His-SUMO2 conjugates were purified with Ni-NTA beads and analyzed by Western blotting with anti-Myc mouse antibody. Expression levels of Myc-tagged MTA1, FLAG-tagged PIAS proteins, and vinculin were detected by immunoblotting with the indicated antibodies. *C*, SENP1 and SENP2 deSUMOylate SUMOylation of MTA1 *in vitro*. FLAG-tagged WT SENP1, SENP2, or SENP3, or their catalytically inactive mutants generated by unlabeled *in vitro* translation, were mixed with *in vitro* SUMOylated MTA1. The reaction products were resolved by SDS-PAGE and visualized by autoradiography. Western blotting with anti-FLAG mouse antibody served as a loading control for the proteases. *D*, SENP1 and SENP2 deSUMOylate SUMOylation of MTA1 *in vivo*. COS-1 cells were co-transfected with the indicated expression vectors. HA-His-SUMO2 conjugates were purified with Ni-NTA beads and analyzed by Western blotting with anti-Myc mouse antibody. Expression levels of Myc-tagged MTA1, FLAG-tagged SENP proteins, and vinculin were detected by immunoblotting with the indicated antibodies.

gation efficiency than PIAS1 and PIASy (Fig. 3*B*, *lanes 3* and *5*). Furthermore, the interactions of the indicated PIAS proteins with MTA1 were validated by co-immunoprecipitation (supplemental Fig. S2*A*).

SENP1 and SENP2 May Function as DeSUMOylation Enzymes for MTA1—Given that SUMOylation is a highly dynamic process, we next examined which SUMO-specific isopeptidase might be involved in the deSUMOylation of MTA1. In the SENP family, SENP1 is located in the nucleus and SENP2 in both the nucleus and the cytoplasm, and SENP3 and SENP5 mainly exert their functions in the nucleolus (5). To analyze directly whether SENP1, SENP2, or SENP3 could catalyze the deSUMOylation of MTA1, an *in vitro* deSUMOylation assay was performed. PreSUMOylated MTA1 was incubated with the WT or catalytically inactive mutant forms of SENP1, SENP2, or SENP3. We found that the SUMO2 conjugates were significantly reduced under conditions of supplementation with SENP1-WT or SENP2-WT proteins (Fig. 3*C*, *lanes 3* and *5*) but not in the reactions with the addition of their inactive mutants (Fig. 3*C*, *lanes 4* and *6*). In contrast, neither SENP3-WT nor its inactive mutant could decrease the SUMOylation of MTA1 (Fig. 3*C*, *lanes 7* and *8*). Moreover, similar results were observed *in vivo* when we co-transfected Myc-tagged MTA1 with HA-His-tagged SUMO2 expression vectors, alone or together with FLAG-tagged SENP1–3 WT or their mutant constructs (Fig. 3*D*). Furthermore, the interactions of SENP1 or SENP2 with MTA1 were validated by co-immunoprecipitation (supplemental Fig. S2*B*). Collectively, these results suggest that SENP1 and SENP2, but not SENP3, may function as deSUMOylation enzymes for MTA1.

SUMOylation Does Not Affect the Protein Stability of MTA1—Given that the elevated levels of MTA1 are closely correlated with tumor progression and metastasis (9), we next examined whether SUMO modification could affect the protein stability of MTA1. To this aim, we first examined the stability of endogenous MTA1 in MCF-7 cells overexpressing empty vector, HA-His-tagged SUMO2 or FLAG-tagged UBC9, PIAS3, or SENP1, respectively. We found that the induced expression of SUMO2,

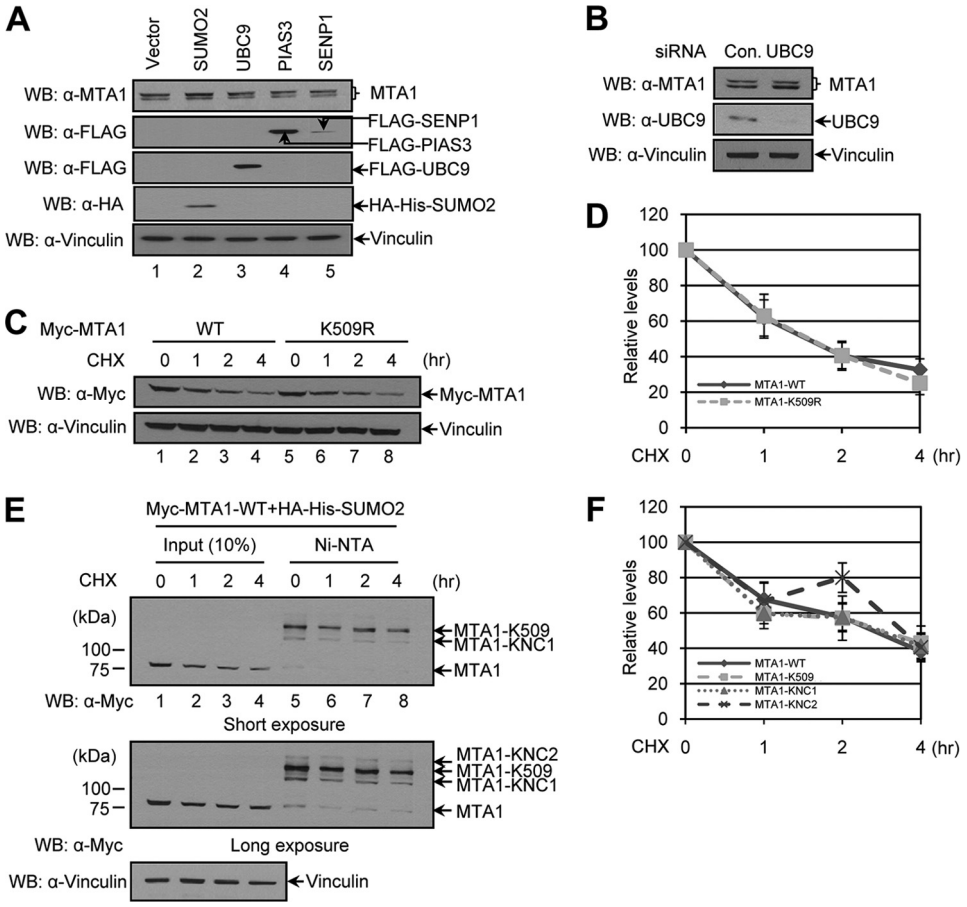

FIGURE 4. **SUMOylation does not affect the protein stability of MTA1.** *A*, MCF-7 cells were transfected with one of the following constructs: control vector, HA-His-tagged SUMO2, or FLAG-tagged UBC9, PIAS3, or SENP1. Cell lysates were analyzed by Western blotting (*WB*) with anti-MTA1 rabbit antibody. Expression levels of HA-tagged SUMO2, FLAG-tagged proteins, and vinculin were detected by immunoblotting with the indicated antibodies. *B*, MCF-7 cells were transfected with control or UBC9 siRNA. Cells lysates were analyzed by Western blotting with anti-MTA1 rabbit antibody. Expression levels of UBC9 and vinculin are shown. *C*, MCF-7 cells were transfected with the construct of Myc-tagged MTA1-WT or MTA1-K509R mutant and treated with cycloheximide (*CHX*, 100 μg/ml) for the indicated time points. Cell lysates were analyzed by Western blotting with anti-Myc mouse antibody. Expression levels of vinculin are shown as loading control. *D*, the data from *C* are shown in graph form with S.D. ($n = 3$). *E*, COS-1 cells were co-transfected with Myc-tagged MTA1 and HA-His-tagged SUMO2 constructs and treated with cycloheximide as described in *C*. HA-His-SUMO2 conjugates were purified with Ni-NTA beads and analyzed by Western blotting with anti-Myc mouse antibody. Expression levels of Myc-tagged MTA1 and vinculin are shown as *input*. *KNC1* and *KNC2* represent the SUMOylated MTA1 in which lysine residues in non-consensus sites are modified by SUMO2. *F*, the data from *E* are shown in graph form with S.D. ($n = 3$).

UBC9, PIAS3, or SENP1 did not change the protein levels of endogenous MTA1 (Fig. 4*A*). Consistently, knockdown of endogenous UBC9 in MCF-7 cells also did not affect the protein levels of endogenous MTA1 (Fig. 4*B*).

Next, we tested whether SUMOylation and ubiquitination could share the same lysine residue, Lys-509, by comparing the stability between MTA1-WT and the MTA1-K509R mutant. MCF-7 cells were transfected with Myc-tagged MTA1-WT or the MTA1-K509R mutant construct and then treated with cycloheximide to block new protein synthesis. Cells were harvested at various times, and the protein levels of MTA1 were analyzed by Western blotting. As shown in Fig. 4, *C* and *D*, both MTA1-WT and its K509R mutant had very similar half-lives.

Following these observations, we next attempted to test the stability of the SUMOylated MTA1. For this purpose, we co-transfected COS-1 cells with Myc-tagged MTA1-WT and HA-His-tagged SUMO2 constructs. After transfection, cells were treated with cycloheximide and harvested at various times. The SUMOylated MTA1 was recovered on Ni-NTA beads and analyzed by Western blotting. We found that the majority of SUMOylated MTA1 showed very similar half-lives as free MTA1 (Fig. 4, *E* and *F*). Thus, based on all of the above results, we have concluded that SUMOylation, including global SUMOylation and MTA1 SUMOylation itself, would unlikely affect the stability of MTA1.

MTA1 Directly and Noncovalently Binds to SUMO1 or SUMO2—The feature of SUMO that allows it to modulate protein activity through noncovalent binding prompted us to examine whether MTA1 could bind to SUMO paralogs noncovalently. The MCF-7 cell extracts were incubated with nonconjugatable forms of GST-tagged SUMO1 (GST·SUMO1GA) or SUMO2 (GST·SUMO2GA) or control GST affinity resins. The proteins were analyzed by Western blotting with anti-MTA1 rabbit antibody. As shown in Fig. 5*A* (*lanes 3* and *4*), both SUMO1 and SUMO2 interact with MTA1. Moreover, by performing GST pull-down assay with ^{35}S-labeled, *in vitro* translated MTA1, we found that SUMO paralogs could physically bind to MTA1 (Fig. 5*B*, *lanes 4* and *5*). In addition, we also confirmed the interaction between UBC9 and MTA1 (Fig. 5*A*, *lane 2*, and *B*, *lane 3*).

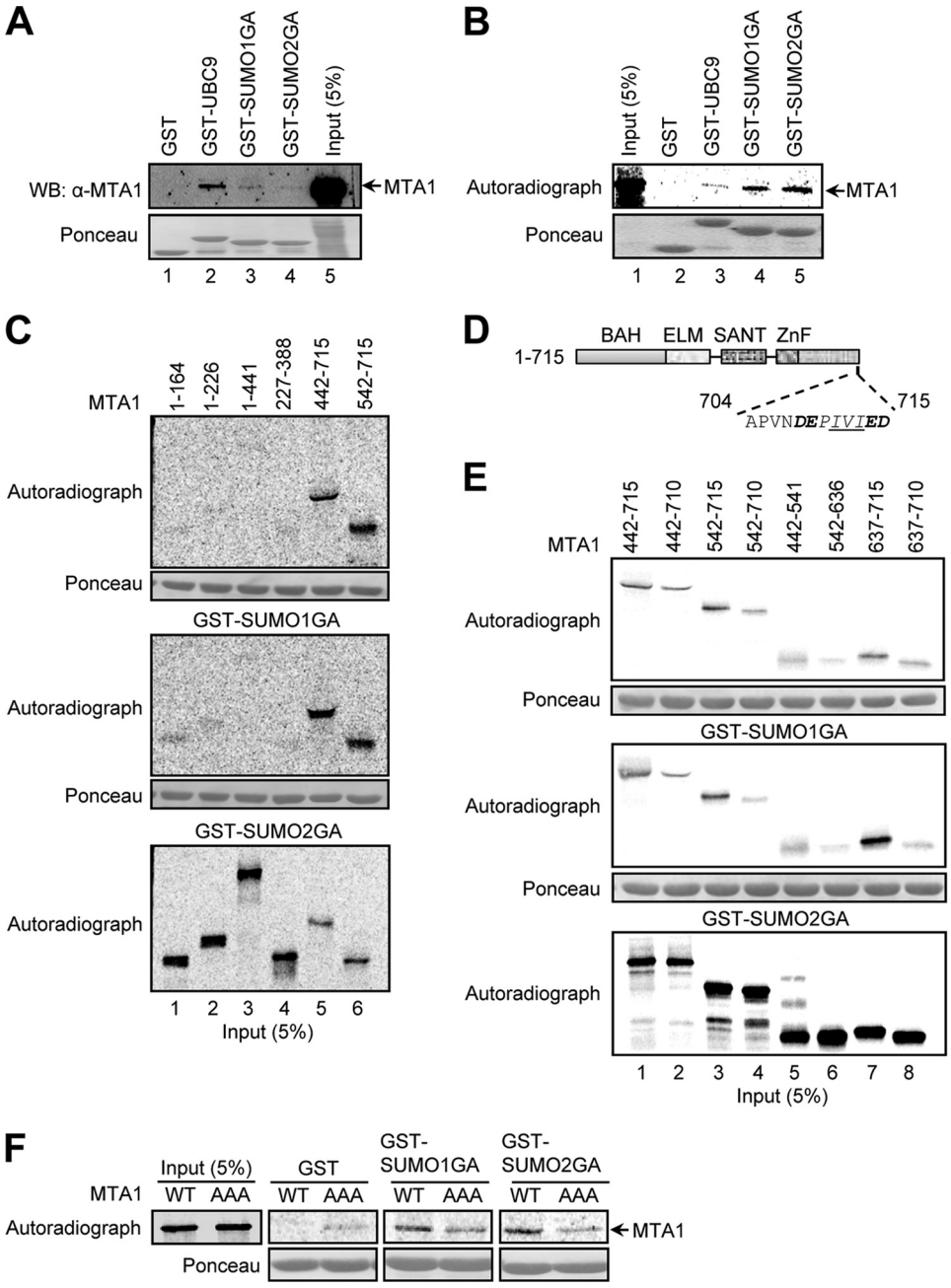

FIGURE 5. **Identification of the SUMO-interacting motif (SIM) in MTA1.** *A*, MCF-7 cell lysates were incubated with GST, GST-tagged UBC9, or nonconjugatable forms of SUMO1 (*GST-SUMO1GA*) or SUMO2 (*GST-SUMO2GA*). Proteins retained on glutathione-Sepharose beads were analyzed by Western blotting (*WB*) with anti-MTA1 rabbit antibody. The same blot was stained by Ponceau staining to detect GST control or GST fusion proteins. *B*, *in vitro* translated, ^{35}S-labeled MTA1-WT was pulled down by GST or the indicated GST fusion proteins as described in *A*. The proteins were resolved by SDS-PAGE and visualized by autoradiography. GST or GST fusion proteins were detected by Ponceau staining. *C* and *E*, *in vitro* translated, ^{35}S-labeled MTA1 fragments were pulled down by the indicated GST fusion proteins. The reaction products were analyzed as described in *B*. GST or GST fusion proteins were detected by Ponceau staining. *D*, schematic drawing of putative SIM (*italic*) in MTA1 is shown. The hydrophobic core (*underlined*) and flanked acidic amino acids (*bold*) in SIM are indicated. *F*, *in vitro* translated, ^{35}S-labeled MTA1-WT or its I711A/V712A/I713A (*AAA*) mutant was pulled down by the indicated GST fusion proteins. The reaction products were analyzed as described in *B*. GST or GST fusion proteins were detected by Ponceau staining.

To identify the SIM in MTA1, a series of MTA1 truncation mutants were constructed and generated by ^{35}S-labeled *in vitro* transcription/translation. The results from the GST pulldown assays indicated that the region between amino acids 542 and 715 of MTA1 displayed robust binding to either SUMO1 or SUMO2 (Fig. 5*C*). Although the last eight amino acids in this region (Fig. 5*D*, *DEPIVIED*) resembled the best featured SIM ((V/I)*X*(V/I)(V/I) flanked with acidic amino acids), we were not sure whether this was the only SIM in MTA1, as there are several different types of SIM that have been reported (20–22). To address this question, we further produced several truncation mutants with or without the last five amino acids (IVIED) to identify the SIM in MTA1. GST pulldown assays showed that the absence of this motif dramatically reduced the binding ability of MTA1 fragments with SUMO proteins (Fig. 5*E*). Furthermore, triple mutations in the hydrophobic core (I711A/V712A/

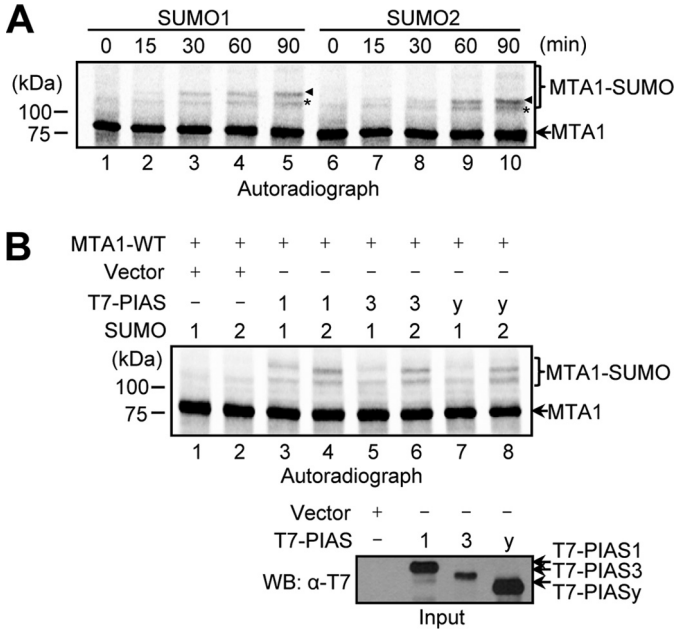

FIGURE 6. **PIAS proteins may participate in paralog-selective SUMOylation of MTA1.** *A*, UBC9 and SIM are not responsible for paralog-selective SUMOylation of MTA1. MTA1-WT was generated by ^{35}S-labeled *in vitro* translation and incubated in SUMOylation reactions containing either SUMO1 or SUMO2. The reactions were stopped at the indicated time points. SUMOylation products were analyzed by autoradiography. The bands representing SUMO conjugation on Lys-509 and the lysine residue within the non-consensus site are indicated by an *arrowhead* and an *asterisk*, respectively. *B*, PIAS proteins enhance SUMO2 modification of MTA1. Unlabeled, *in vitro* translated PIAS1, PIAS3, or PIASy was incubated with ^{35}S-labeled, *in vitro* translated MTA1 in SUMOylation reactions containing either SUMO1 or SUMO2. The reaction products were resolved by SDS-PAGE and directly detected by autoradiography. Western blot (*WB*) with anti-T7 rabbit antibody showed the amounts of PIAS proteins used in this assay.

I713A, referred to here as AAA) significantly impaired the interactions of MTA1 with SUMO1 or SUMO2 as compared with MTA1-WT (Fig. 5*F*). Together, these results define a SIM in MTA1 in which a hydrophobic core is required for high affinity binding to SUMO proteins.

PIAS Proteins May Be Involved in Paralog-selective SUMOylation of MTA1—Because both UBC9 and SIM are involved in paralog-selective SUMOylation (8, 23, 24), and endogenous MTA1 was only modified by SUMO2/3 (Fig. 1*D*), we explored the possibility of whether the noted paralog-selective SUMOylation of MTA1 depended on UBC9, SIM, or both. As shown in Fig. 6*A*, SUMO1 and SUMO2 showed similar modification efficiency at the indicated time points in the reactions containing only E1 and E2 enzymes, suggesting that paralog-selective SUMOylation of MTA1 is UBC9/SIM-independent. In addition, we found that MTA1 equally accepted SUMO proteins on lysine residues within either the SUMO consensus (Fig. 6*A*, *arrowhead*) or non-consensus site (Fig. 6*A*, *asterisk*; from 0 to 60 min).

Next, we introduced PIAS proteins into the reactions to examine the roles of PIAS proteins in SUMO paralog selection. Interestingly, we found that MTA1 preferred to be modified by SUMO2 in the presence of the PIAS proteins (Fig. 6*B*, *lanes 3*, *5*, and *7 versus lanes 4*, *6*, and *8*). These findings collectively suggest that PIAS proteins, but not UBC9 or SIM in MTA1, are required for paralog-selective SUMOylation of MTA1.

SIM Is Crucial for the Efficient SUMOylation of MTA1—The notion that functional SIM may be required for SUMOylation as is the case for Daxx and USP25 (3, 8) led us to investigate whether the SUMO-SIM interaction would contribute to the SUMOylation of MTA1. *In vitro* SUMOylation analysis showed that a single mutation in the SIM impaired SUMOylation of MTA1 (Fig. 7*A*, *lanes 3–7*), and triple mutations in the hydrophobic core of the SIM (AAA) abolished SUMO2 conjugation of MTA1 (Fig. 7*A*, *lane 9*). Moreover, the high concentration of free SUMO2 interrupted SUMOylation of MTA1, probably because free SUMO2 can compete with UBC9·SUMO2 complex in the recognition of MTA1 (Fig. 7*B*). Notably, MTA1-WT and the MTA1-AAA mutant bound to GST-UBC9 with equal efficiency in the GST pulldown assay (Fig. 7*C*, *lanes 7* and *9*). However, the MTA1-K509R mutant showed a slightly reduced binding with GST-UBC9 (Fig. 7*C, lane 8*). These results suggest that the reduced SUMOylation of MTA1 is probably not due to the disruption of the structural integrity of MTA1 or the interruption of the binding between UBC9 and MTA1.

Because E3 ligase functions as a platform to pull the UBC9·SUMO complex and the substrate together to facilitate SUMOylation, we next investigated whether the SUMO-SIM interaction was required for the enhanced SUMOylation of MTA1 by PIAS3. Interestingly, a single mutation of an acidic amino acid in the SIM did not affect the SUMOylation of MTA1 in the presence of PIAS3 (Fig. 7*D*, *lanes 7* and *8*). However, PIAS3 could not restore the reduced SUMOylation caused by the mutations in the hydrophobic core of SIM (Fig. 7*D*, *lanes 4–6*, *9*, and *10*), and the most significant reduction of SUMOylation was observed with the MTA1-AAA mutant (Fig. 7*D*, *lane 10*). Importantly, the result that triple mutations in the hydrophobic core reduced the SUMOylation of MTA1 was recapitulated *in vivo* by co-expressing Myc-tagged MTA1-WT or MTA1-AAA and HA-His-tagged SUMO2 in COS-1 cells (Fig. 7*E, lane 4 versus 6*). Moreover, to unequivocally confirm the importance of the SUMO-SIM interaction in the SUMOylation of MTA1, the lysine residues in SUMO2 (Lys-33, Lys-35, and Lys-42), which are reported to play vital roles in binding with SIM (25), were mutated to glutamic acid. Myc-tagged MTA1-WT was co-expressed with HA-His-tagged SUMO2-WT or its mutants in COS-1 cells. Compared with the WT, SUMO2 mutants significantly impaired SUMOylation of MTA1 (Fig. 7*F*, *lane 1 versus lanes 2–4*). Thus, these data demonstrate that the SUMO-SIM interaction is crucial for the efficient SUMOylation of MTA1.

Both Lys-509 and SIM Are Required for Full Co-repressive Activity of MTA1—As SUMOylation does not affect MTA1 stability (Fig. 4) and MTA1 functions as a co-repressor in estrogen-responsive element (ERE)-driven gene repression (10), we next examined whether SUMOylation and SIM would participate in MTA1-mediated gene repression. Because 17β-estradiol can affect the SUMOylation of AIB1 and ERα (26, 27), we first investigated whether the level of SUMOylation of MTA1 would be affected by 17β-estradiol treatment. Myc-tagged MTA1 was co-expressed with HA-His-tagged SUMO2 alone or together with FLAG-tagged UBC9 or PIAS3 in MCF-7 cells in the absence or presence of 17β-estradiol for 3 h. We found that 17β-estradiol treatment did not affect the SUMOylation of

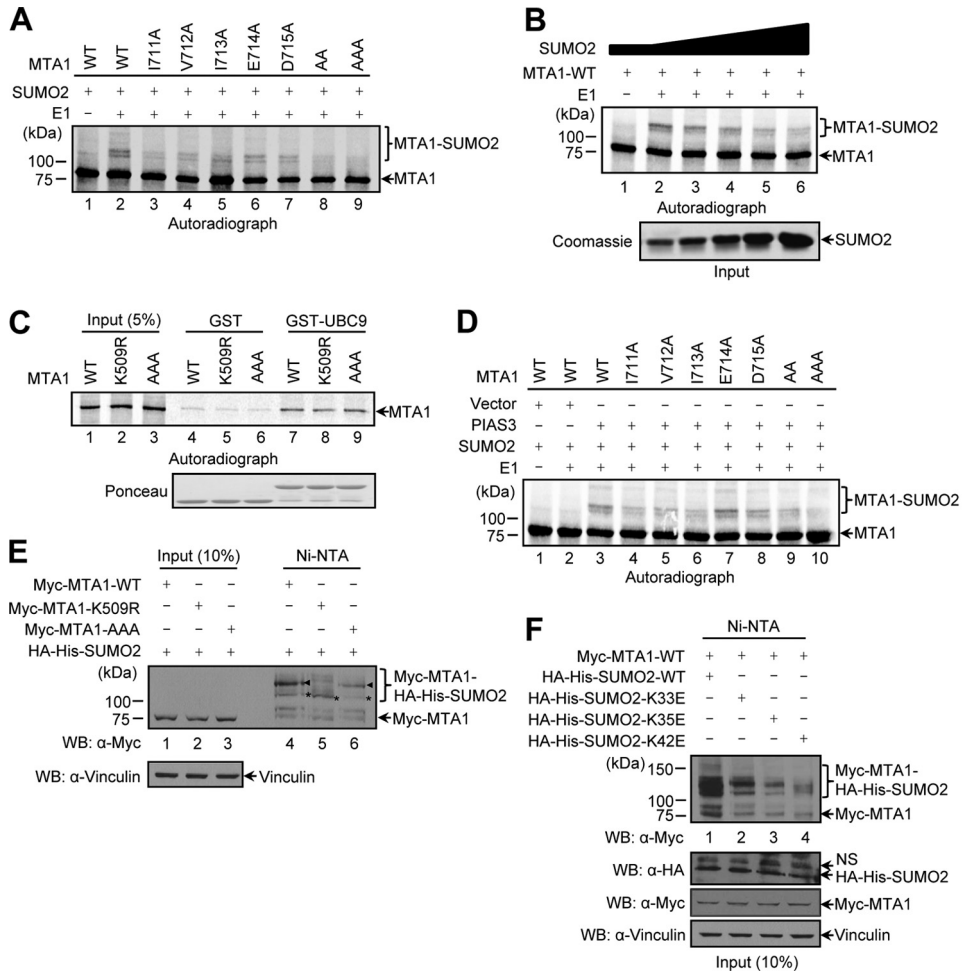

FIGURE 7. **SIM is crucial for the efficient SUMOylation of MTA1.** *A*, *in vitro* translated, ^{35}S-labeled MTA1-WT or its SIM mutants were incubated in SUMOylation reactions containing SUMO2 and 0.25 μg of GST-UBC9. The reaction products were resolved by SDS-PAGE and visualized by autoradiography. *AA* represents the I711A/V712A mutant of MTA1; *AAA* represents the I711A/V712A/I713A mutant of MTA1. *B*, MTA1-WT was generated by ^{35}S-labeled *in vitro* translation and incubated in SUMOylation reactions containing 0.25 μg of GST-UBC9 together with increasing amounts of SUMO2 (*lane 1*, 0.25 μg; *lanes 2–6*, 0.25, 0.5, 1, 2, and 4 μg, respectively). The reaction products were analyzed as described in *A*. Coomassie staining of the gel showed the input of SUMO2 used in the assay. *C*, GST pulldown assays were performed by incubating *in vitro* translated, ^{35}S-labeled MTA1-WT, MTA1-K509R, or MTA1-AAA mutant with GST-control or GST-UBC9 fusion proteins. The reaction products were analyzed as described in *A*. Ponceau staining showed the indicated GST fusion proteins used for each binding assay. *D*, unlabeled, *in vitro* translated PIAS3 was incubated with ^{35}S-labeled, *in vitro* translated MTA1-WT or its SIM mutants in SUMOylation reactions containing SUMO2 and 0.03 μg of GST-UBC9. The reaction products were analyzed as described in *A*. *E* and *F*, COS-1 cells were co-transfected with the indicated expression vectors. HA-His-SUMO2 conjugates were purified with Ni-NTA beads and analyzed by Western blotting (*WB*) with anti-Myc mouse antibody. Expression levels of Myc-tagged MTA1, HA-His-tagged SUMO2 proteins (*F*), and vinculin were detected with the indicated antibodies. In *E*, the bands representing SUMO2 conjugation on Lys-509 and the lysine residue within the non-consensus site are indicated by *arrowheads* and *asterisks*, respectively. *NS*, nonspecific.

MTA1 (Fig. 8*A*). Similarly, *in vivo* endogenous SUMOylation of MTA1 was not affected upon 17β-estradiol treatment at the indicated time points (Fig. 8*B*). These results suggest that MTA1 undergoes SUMO modification in an estrogen-independent manner.

Next, we investigated the effect of SUMOylation on the expression of *PS2*, a target gene down-regulated by MTA1 (10). We found that knockdown of endogenous UBC9 in MCF-7 cells increased *PS2* mRNA levels as compared with the control (Fig. 8*C*), suggesting that SUMOylation may be involved in MTA1-mediated repression of *PS2* transcription. To test this hypothesis, we next examined whether the disruption or augmentation of global SUMO conjugation would affect the repressive effect of MTA1 on *PS2* promoter activity. In the presence of 10 nM 17β-estradiol, the repression of the *PS2* promoter activity, achieved by overexpression of MTA1-WT, was completely abolished by co-expression of SENP1-WT but not its inactive mutant (Fig. 8*D*). On the other hand, overexpression of SUMO2, UBC9, or PIAS3 along with MTA1-WT further enhanced MTA1-repressed *PS2* promoter activity (Fig. 8*E*). In addition, similar results were observed when using the Gal4–3×ERE luciferase reporter system (supplemental Fig. S3). Therefore, these results clearly demonstrate that SUMOylation enhances the repressive effect of MTA1 on *PS2* promoter activity.

To further examine the effects of SUMO-conjugated Lys-509 and the SUMO-SIM interaction on *PS2* transcriptional activity, MCF-7 cells were co-transfected with the constructs of T7-tagged MTA1-WT, MTA1-K509R, MTA1-AAA, or MTA1-K509R/AAA mutant together with the *PS2*-Luc reporter gene in the presence of 10 nM 17β-estradiol. We found that both the MTA1-K509R and MTA1-AAA mutants

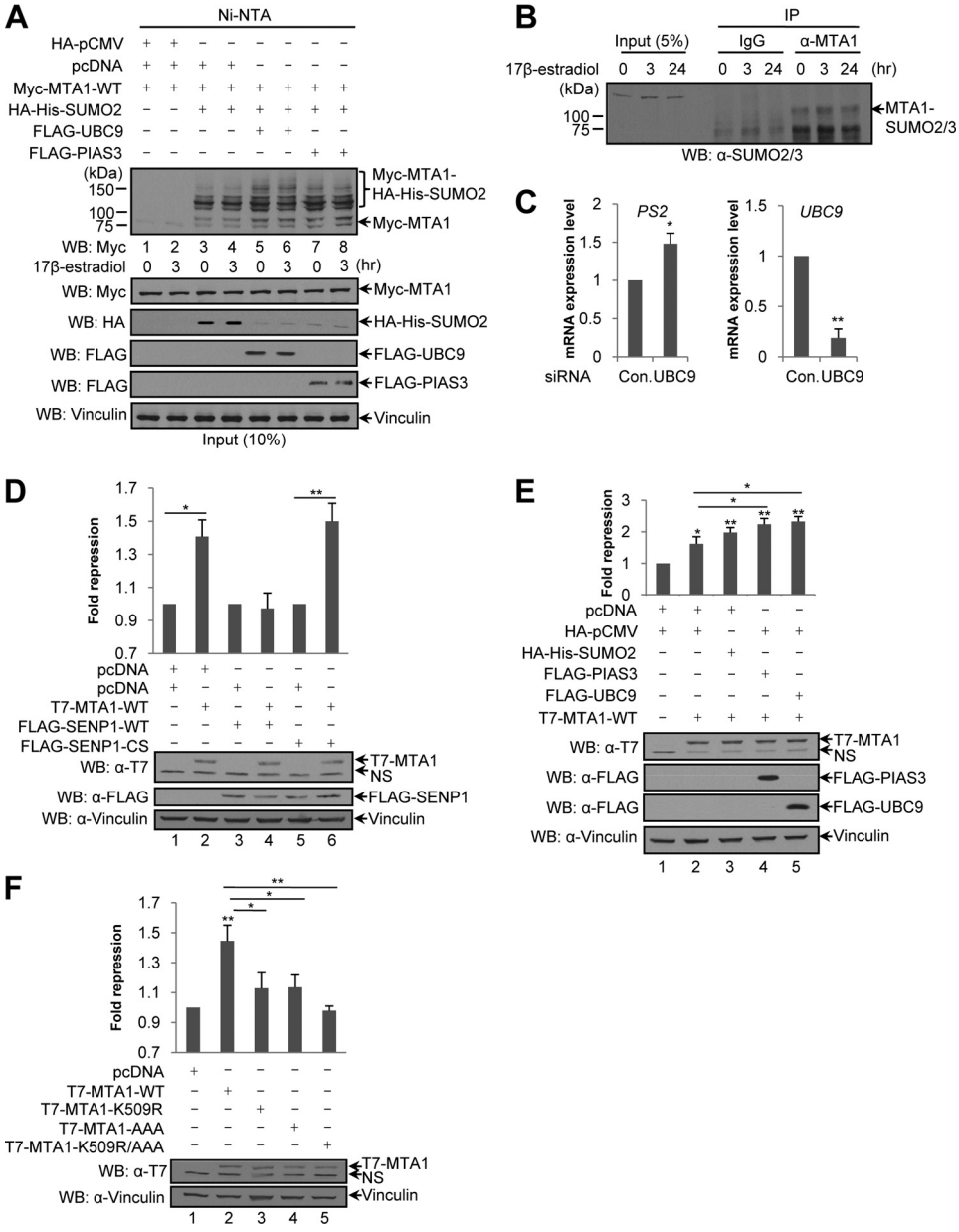

FIGURE 8. **Both Lys-509 and SIM are required for the full co-repressive effect of MTA1 on *PS2* transcription.** *A*, SUMOylation of MTA1 is not affected by 17β-estradiol treatment *in vivo*. MCF-7 cells were co-transfected with various combinations of expression vectors as indicated in figure above. One microgram of HA-His-SUMO2 construct was co-transfected with Myc-tagged MTA1 plasmid, and 0.5 μg of HA-His-SUMO2 construct was co-transfected with Myc-tagged MTA1 plasmid together with FLAG-tagged UBC9 or PIAS3 constructs in MCF-7 cells. Thirty-six hours after transfection, the cells were treated with 10 nM 17β-estradiol and then harvested and lysed after another 3 h. HA-His-SUMO2 conjugates were purified by Ni-NTA beads and analyzed by Western blotting (*WB*) with anti-Myc mouse antibody. Expression levels of Myc-tagged MTA1, HA-tagged SUMO2, FLAG-tagged UBC9 and PIAS3, and vinculin were detected with the indicated antibodies. *B*, endogenous SUMOylation of MTA1 is not affected by 17β-estradiol treatment. MCF-7 cells were treated with 10 nM 17β-estradiol at the indicated time points. MCF-7 cells were harvested under denaturing conditions prior to immunoprecipitation (*IP*) with anti-MTA1 rabbit antibody followed by immunoblotting with anti-SUMO2/3 rabbit antibody. *C*, quantitative RT-PCR analysis of *SUMO2* (*left*) or *UBC9* (*right*) expression in MCF-7 cells transfected with control or UBC9 siRNA. The expression levels of *PS2* or *UBC9* in controls were set to 1.0. *D–F*, MCF-7 cells were transiently co-transfected with the *PS2*-Luc reporter gene, pSV-β-galactosidase control vector, and various combinations of expression vectors as indicated in figure above. Twenty-four hours after transfection, the cells were treated with 10 nM 17β-estradiol and then harvested and lysed after another 24 h. The resulting extracts were used for the luciferase activity assay. Luciferase activity was normalized to the β-galactosidase activity. The results were presented as -fold repression of relative luciferase units, and the luciferase activity levels of the samples in the absence of MTA1 were set to 1.0. The expression levels of the indicated proteins are shown as loading control. *NS*, nonspecific. The results represent mean values ± S.D. *p* values were determined using Student's *t* test ($n = 3$); *, $p < 0.05$; **, $p < 0.02$.

(Fig. 8*F*, *lanes 3* and *4*) relieved ~60% of the repressive effect on *PS2* transcription compared with the sample overexpressing MTA1-WT (Fig. 8*F*, *lane 2*). Interestingly, the MTA1-K509R/AAA mutant completely lost the ability to repress *PS2* transcription (Fig. 8*F*, *lane 5*). These data suggest that SUMO conjugation on Lys-509, together with the SUMO-SIM interaction, contributes to the full repressive effect of MTA1 on transcription of the tested target gene, *PS2*.

Both Lys-509 and SIM Are Required to Synergistically Regulate the Recruitment of HDAC2 onto the PS2 Promoter—To better understand the involvement of SUMO2/3 in MTA1-medi-

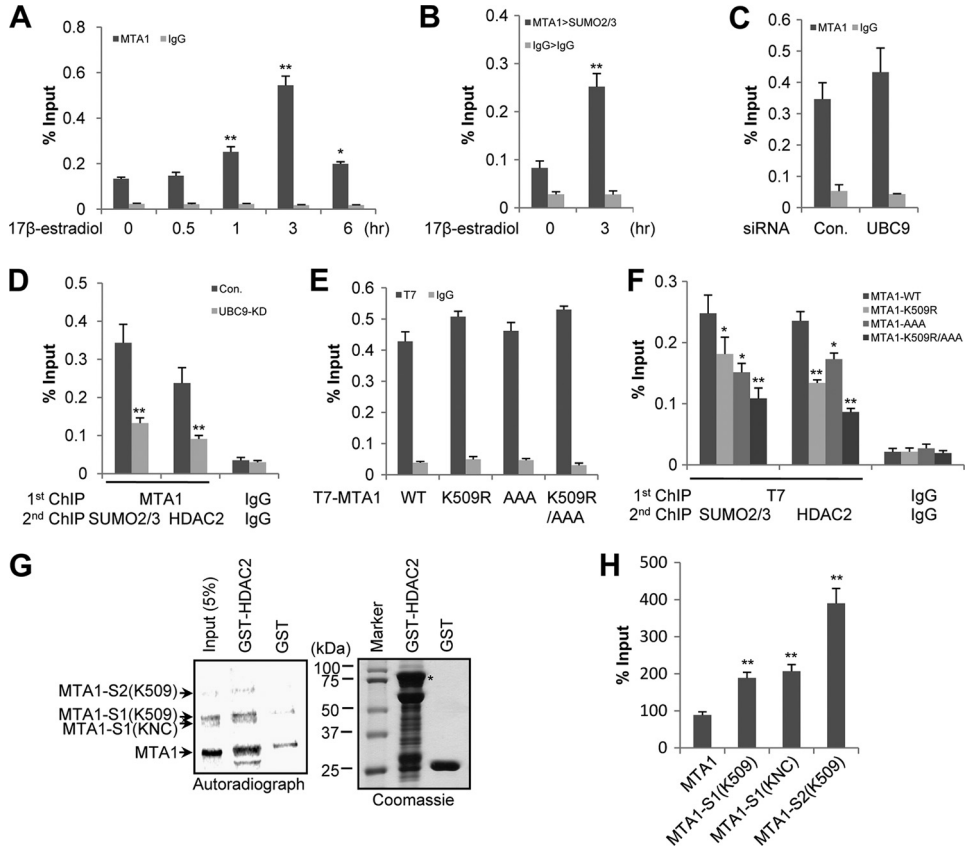

FIGURE 9. **Both Lys-509 and SIM are required for the synergistic regulation of recruitment of HDAC2 onto the *PS2* promoter.** *A*, MCF-7 cells were treated with 10 nM 17β-estradiol at the indicated time points. Then cells were cross-linked and processed for a single-ChIP assay with anti-MTA1 rabbit antibody or control IgG, and quantitative RT-PCR was performed. *B*, MCF-7 cells were treated with or without 10 nM 17β-estradiol for 3 h. Subsequently, the cells were cross-linked and processed for sequential double-ChIP with anti-MTA1 rabbit antibody followed by anti-SUMO2/3 rabbit antibody or double-ChIP with IgG as control. Quantitative RT-PCR was performed. *C* and *D*, MCF-7 cells were transfected with control or UBC9 siRNA for 48 h and treated with 10 nM 17β-estradiol for another 3 h. The cells were then processed for a single-ChIP assay with anti-MTA1 rabbit antibody (*C*) or sequential double-ChIP assays with anti-MTA1 rabbit antibody followed by anti-SUMO2/3 or anti-HDAC2 rabbit antibody (*D*) or ChIP with IgG as control. Quantitative RT-PCR was performed. *E* and *F*, MCF-7 cells were transfected with T7-tagged MTA1-WT, MTA1-K509R, MTA1-AAA, or MTA1-K509R/AAA mutant constructs for 48 h and treated with 10 nM 17β-estradiol for another 3 h. The cells were processed for single-ChIP with anti-T7 mouse antibody (*E*) or sequential double-ChIP assays with anti-T7 mouse antibody followed by anti-SUMO2/3 or anti-HDAC2 rabbit antibody (*F*) or ChIP with IgG as control. Quantitative RT-PCR was performed. The ChIP-quantitative RT-PCR results are shown as a percentage of input with S.D., where % input = $100 \times 2^{\Delta Ct}$ and $\Delta Ct = Ct(Input) - Ct(IP) - 6.644$. *p* values were determined using Student's *t* test ($n = 3$); *, $p < 0.05$; **, $p < 0.02$. *G*, MTA1-WT was generated by ^{35}S-labeled *in vitro* translation and incubated in a SUMOylation reaction containing SUMO2. SUMO2-modified MTA1 was then used in GST pulldown assays with GST or GST-HDAC2 fusion protein. The retained proteins were detected by autoradiography (*left*). Coomassie staining of the gel showed the input of the purified recombinant GST and GST-HDAC2 fusion protein (*asterisk*) used in the assay (*right*). *S1* and *S2* represent MTA1 modified by a mono-SUMO2 molecule or di-SUMO2 molecules, respectively. *KNC* represents MTA1 modified by SUMO2 on the SUMO non-consensus site. *H*, quantification by Photoshop CS5 software of MTA1 species recovered by pulldown *versus* input (% of input band intensity) with S.D.; **, $p < 0.02$ ($n = 3$).

ated gene repression, we first analyzed MTA1 occupancy on the *PS2* promoter by using a ChIP assay. MCF-7 cells were treated with 17β-estradiol at various times. Chromatin was prepared and analyzed by using a single-ChIP assay with anti-MTA1 rabbit antibody. We found that the recruitment of MTA1 onto the *PS2* promoter increased with the treatment of 17β-estradiol. The maximal recruitment of endogenous MTA1 onto the *PS2* promoter, which was about 4-fold higher than without treatment, occurred following 17β-estradiol treatment for 3 h (Fig. 9*A*). These data are supported by the finding that the NuRD complex was recruited to the *PS2* promoter 100–180 min after α-amanitin release and following 10 nM 17β-estradiol treatment (28); thus we used this condition to perform the following ChIP experiments. To test whether SUMO2/3 and MTA1 would form the same complex at the *PS2* promoter, a sequential double-ChIP with anti-MTA1 rabbit antibody followed by anti-SUMO2/3 rabbit antibody was performed in the absence or presence of 10 nM 17β-estradiol for 3 h. We found that not only SUMO2/3 and MTA1 were detected in the same complex at the *PS2* promoter, but also the recruitment of MTA1·SUMO2/3 complex was about 3.3-fold higher than without 17β-estradiol treatment (Fig. 9*B*). Because MTA1 noncovalently bound to SUMO2/3, one possibility is that free SUMO2/3 could form a complex with MTA1 at the *PS2* promoter as well. To address this question, MCF-7 cells transfected with control or UBC9 siRNA were treated with 10 nM 17β-estradiol for 3 h. Then a single-ChIP with anti-MTA1 rabbit antibody and a sequential double-ChIP with anti-MTA1 rabbit antibody followed by anti-SUMO2/3 rabbit antibody were performed. We found that siRNA-mediated UBC9 knockdown slightly increased the recruitment of MTA1 onto the *PS2* promoter (Fig. 9*C*), whereas it decreased about 64% of the recruitment of the MTA1·SUMO2/3 complex onto the *PS2* promoter (Fig. 9*D*). Considering the knockdown efficiency and background of IgG,

it was reasonable to conclude that the majority of SUMO2/3 in the MTA1·SUMO2/3 complex at the *PS2* promoter was the one conjugated to MTA1 or another protein but not free SUMO2/3 form.

Because HDAC2, another component in the NuRD complex, is reportedly involved in repressing *PS2* transcription (10), we next investigated whether SUMO modification could affect the binding of HDAC2 with MTA1 at the *PS2* promoter. As shown in Fig. 9*D*, we found that siRNA-mediated UBC9 knockdown resulted in a loss of 60% of the HDAC2 binding with MTA1 at the *PS2* promoter compared with the control. These results clearly suggest that the binding of HDAC2 with MTA1 at the *PS2* promoter is in a SUMOylation-dependent manner.

To further examine whether SUMOylation of MTA1 on Lys-509 and the SUMO-SIM interaction could affect the recruitment of HDAC2 onto the *PS2* promoter, MCF-7 cells were transfected with T7-tagged MTA1-WT, MTA1-K509R, MTA1-AAA, or MTA1-K509R/AAA constructs under treatment with 10 nM 17β-estradiol for 3 h. Chromatin was prepared and analyzed by a single-ChIP with anti-T7 mouse antibody and sequential double-ChIP assays with anti-T7 mouse antibody followed by anti-SUMO2/3 or anti-HDAC2 rabbit antibody. Although the recruitments of MTA1-WT and its mutants onto *PS2* promoter did not change significantly (Fig. 9*E*), the MTA1-K509R, MTA1-AAA, and MTA1-K509R/AAA mutants lost about 27, 39, and 56% of their SUMO2/3 association and 43, 27, and 63% of their HDAC2 binding at the *PS2* promoter, respectively (Fig. 9*F*). These results still do not rule out the possibility that free SUMO2/3 could bind to MTA1 at the *PS2* promoter, but at least we can conclude that SUMO2/3 is covalently bound to MTA1 at the *PS2* promoter because the MTA1-K509R mutant lost about 27% SUMO2/3 association. Taken together, these results not only support the notion that the binding of HDAC2 and MTA1 at the *PS2* promoter is SUMOylation-dependent but also suggest that SUMO conjugation at Lys-509 together with SIM shows a synergistic role in the recruitment of HDAC2 onto the *PS2* promoter. Furthermore, when performing a GST pulldown assay, we found that HDAC2 preferentially bound to SUMOylated MTA1 (Fig. 9, *G* and *H*), suggesting that SUMOylated MTA1 may interact directly with HDAC2 but not through other factors in the Mi-2·NuRD complex.

MTA1 May Up-regulate the Expression of SUMO2 via Interaction with Pol II and SP1 at the SUMO2 Promoter—When we examined the global SUMO conjugation using mouse embryonic fibroblasts (MEFs), a significant decrease in SUMO2/3 conjugates, but not SUMO1 conjugates, was observed in MTA1 knock-out ($MTA1^{-/-}$) MEFs compared with that in WT MEFs (Fig. 10*A*). This reduction may not have been from the reduced SUMO conjugation efficiency, because free SUMO2 but not SUMO3 protein levels were dramatically decreased in $MTA1^{-/-}$ MEFs (Fig. 10*A*). Moreover, siRNA-mediated MTA1 knockdown also reduced the protein levels of SUMO2 in MCF-7 cells (Fig. 10*B*). However, we could not detect the reduction of the total SUMO2/3 conjugates, probably because this transient decrease in SUMO2 protein caused by the knockdown of MTA1 was not enough to affect the global SUMO2 conjugation.

To examine whether MTA1 could up-regulate *SUMO2* at the transcriptional level, we measured the mRNA expression levels of the *SUMO2* gene in $MTA1^{+/+}$ and $MTA1^{-/-}$ MEFs using quantitative RT-PCR. We found that, concomitant with reduced SUMO2 protein levels in $MTA1^{-/-}$ MEFs relative to $MTA1^{+/+}$ (Fig. 10*A*), *SUMO2* mRNA expression levels decreased significantly in $MTA1^{-/-}$ MEFs compared with that in the $MTA1^{+/+}$ MEFs (Fig. 10*C*). Consistent with the above results, knockdown of MTA1 by specific siRNA also decreased the *SUMO2* mRNA expression levels compared with the control (Fig. 10*D*). Therefore, the above data indicate that MTA1 could up-regulate the expression of *SUMO2*, at least at the transcriptional level.

Next, we investigated whether MTA1 could associate with the *SUMO2* promoter using a ChIP-based promoter walk assay (Fig. 10*E*). We found that MTA1 was indeed recruited to the human *SUMO2* promoter at a region encompassing residues −2576 to −2806 (Fig. 10*F*). Because Pol II controls gene transcription, we then examined whether MTA1 could form the complex with Pol II at this region using a sequential double-ChIP with anti-MTA1 rabbit antibody followed by anti-Pol II rabbit antibody. As shown in Fig. 10*G*, we found that Pol II could be recruited to the same region and form the same complex with MTA1. Moreover, an attempt to find the putative activator binding site led to the identification of the SP1 binding motif in this region. Results from both the single- and sequential double-ChIP showed that the MTA1·SP1 complex was recruited to this region (Fig. 10, *H* and *I*). Therefore, all of these data suggest that MTA1 may up-regulate the expression of *SUMO2* via interaction with Pol II and SP1 at the *SUMO2* promoter. Finally, *MTA1* exhibited a positive correlation with *SUMO2* in breast cancer tissue samples (Fig. 10*J*).

Because SUMOylation enhanced MTA1-mediated repression, we next investigated whether SUMOylation of MTA1 or SUMO-SIM interaction was involved in the up-regulation of *SUMO2* by performing a sequential ChIP. However, we could not detect recruitment of the MTA1·SUMO2/3 complex onto the *SUMO2* promoter (supplemental Fig. S4), suggesting that SUMO may not participate in MTA1-mediated transactivation of *SUMO2*.

DISCUSSION

In the present study, we have reported for the first time that MTA1 is SUMOylated at Lys-509 within the SUMO consensus site and defined a functional SUMO-interacting motif at its C terminus that is required for the efficient SUMOylation of MTA1. Interestingly, SUMOylation of MTA1 at Lys-509 together with SIM may synergistically regulate MTA1-mediated transcriptional repression of *PS2* by recruiting HDAC2 onto the *PS2* promoter. In addition, MTA1 up-regulates the expression of *SUMO2*. Our findings not only have provided novel mechanistic insights into the regulation of the transcriptional repressor function of MTA1 by SUMOylation and SIM but also have discovered a potential upstream regulator for the SUMOylation pathway.

Roles of SIM in SUMO Modification of MTA1—In general, SUMO conjugation to target proteins takes place at a so-called consensus motif, φK*X*E. UBC9 directly recognizes such a motif

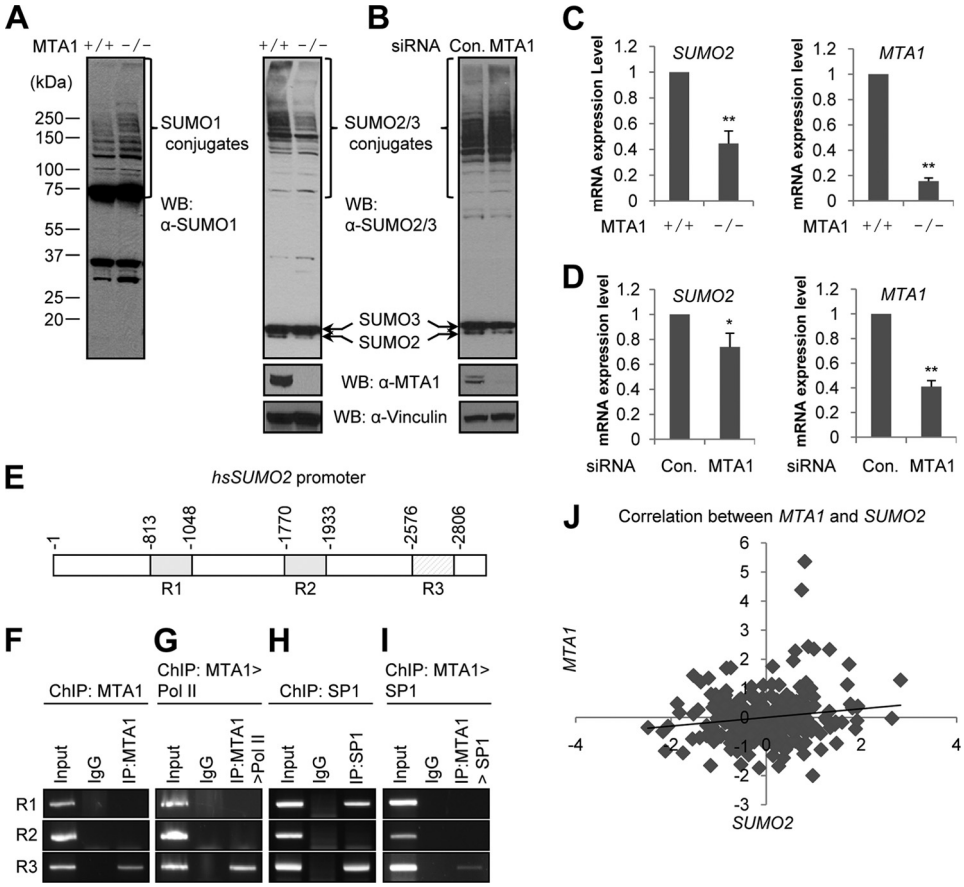

FIGURE 10. **MTA1 may up-regulate the expression of *SUMO2* via interaction with Pol II and SP1.** *A* and *B*, Western blot (*WB*) analysis of SUMO2 expression in the MTA1$^{+/+}$ and MTA1$^{-/-}$ MEFs (*A*) or MCF-7 cells treated with control or MTA1 siRNA (*B*). Expression levels of SUMO1, MTA1, and vinculin were detected with the indicated antibodies. *C* and *D*, quantitative RT-PCR analysis of *SUMO2* or *MTA1* expressions in the MTA1$^{+/+}$ and MTA1$^{-/-}$ MEFs (*C*) or MCF-7 cells treated with control or MTA1 siRNA (*D*). The expression levels of *SUMO2* or *MTA1* in MTA1$^{+/+}$ MEFs or MCF-7 control cells are set to 1.0. The results were the mean values ± S.D. *p* values were determined using Student's *t* test ($n = 3$); *, $p < 0.05$; **, $p < 0.02$. *E*, binding region of MTA1 on human *SUMO2* promoter. *F*, single-ChIP analysis of the recruitment of MTA1 onto *SUMO2* promoter with anti-MTA1 rabbit antibody. *G*, double-ChIP analysis of the recruitment of the MTA1·Pol II complex onto the *SUMO2* promoter with anti-MTA1 rabbit antibody followed by anti-Pol II rabbit antibody. *H*, single-ChIP analysis of the recruitment of SP1 onto the *SUMO2* promoter with anti-SP1 rabbit antibody. *I*, double-ChIP analysis of the recruitment of MTA1·SP1 complex onto the *SUMO2* promoter with anti-MTA1 rabbit antibody followed by anti-SP1 rabbit antibody. *J*, correlation of transcript levels between *MTA1* and *SUMO2* (*r* represents the Pearson's correlation coefficient; $r = 0.15$, $p = 0.01706$).

and transfers the SUMO moiety to the lysine residue embedded in this motif. However, there are also examples of proteins with SUMO conjugation occurring within the non-consensus site, such as BLM, USP25, and Daxx, in which SIM is believed to be required for efficient SUMO modification (3, 8, 24). MTA1 contains both SUMO consensus and non-consensus sites, which accept SUMO1 and SUMO2 with equal efficiency (Fig. 6*A*). Mutation of SIM globally decreased SUMOylation of MTA1 without lysine residue preference (Fig. 7). Our findings suggest that the targeting of the UBC9·SUMO complex to lysine residues may be largely dependent on the SIM of MTA1 but not UBC9. Interestingly, the prediction of the MTA1 secondary structure reveals that SIM is embedded in the coil-tail (supplemental Fig. S5). Given the importance of the SIM in SUMOylation of MTA1, it is possible that this coil-tail structure may confer on the SIM, which is loaded with the UBC9·SUMO complex through the SUMO-SIM interaction, more flexibility to access potential SUMO conjugation sites and then to achieve SUMOylation of MTA1. In fact, we mutated several lysine residues located either close to or far from the SIM along with K509R. However, none of these mutants showed less SUMO conjugation than the MTA1-K509R mutant alone (Fig. 2*C*). Thus, one plausible explanation is that SUMO modification of MTA1 at non-consensus sites may be promiscuous and that mutating one preferred site would result in modification at an alternative site, as is the case with BLM or Daxx (3, 24).

Multiple mechanisms can be proposed in paralog-selective SUMO modification. Protection from isopeptidase-mediated deconjugation regulates paralog-selective SUMOylation of RanGAP1 (29). UBC9·SUMO1 thioester could be recruited to RanBP2 via SUMO1 in the absence of strong binding between UBC9 and RanBP2 (30). In addition, the SIM is a determinant of SUMO paralog selection in substrates (8, 24). In the present study, we found that preferential modification of MTA1 by SUMO2 may be determined by PIAS proteins but not by UBC9 or the SIM of MTA1. However, the underlying mechanism involved is unclear. Considering that both SUMO1 and SUMO2 could be conjugated to the substrates by PIAS proteins (4), we can rule out the possibility that the SIM of PIAS protein could contribute to the paralog-selective SUMOylation of MTA1. Thus, one possible reason could be that the conforma-

tion of UBC9·SUMO2 thioester bond complex may be more suitable for interaction with PIAS proteins and MTA1 to facilitate SUMOylation of MTA1 compared with UBC9·SUMO1 complex.

SUMO Regulates MTA1-mediated Transcriptional Repression—During the course of investigating the role of SUMOylation in regulating MTA1 function, we discovered that SUMOylation did not affect the protein stability of MTA1 (Fig. 4), but SUMO conjugation on Lys-509 together with SIM synergistically regulates the transcriptional repressor function of MTA1 (Fig. 8*F*). Because the NuRD complex is recruited onto the *PS2* promoter upon 17β-estradiol treatment to remove ERα or other transcription factors for creating a silenced chromatin environment (28), and the recruitment of HDAC2 at *PS2* promoter has been reported (10), we reasoned that SUMO might facilitate the interaction between HDAC2 and MTA1 at the *PS2* promoter. That was indeed the case, as we found that, at the *PS2* promoter, knockdown of UBC9 decreased the binding of HDAC2 with MTA1 (Fig. 9*D*), and all three MTA1 mutants (MTA1-K509R, MTA1-AAA and MTA1-K509R/AAA) exhibited less binding ability with HDAC2 compared with MTA1-WT (Fig. 9*F*). Moreover, HDAC2 preferentially bound to SUMOylated MTA1 upon performing a GST pulldown assay (Fig. 9, *G* and *H*). These data clearly indicate that the function of SUMOylation of MTA1, at least in part, may contribute to stabilizing the formation of MTA1·HDAC2 complex.

On the other hand, we found that the recruitment of MTA1 and MTA1·SUMO2/3 complex onto the *PS2* promoter showed a similar ratio after 17β-estradiol treatment for 3 h (Fig. 9, *A* and *B*, 4-fold *versus* 3.3-fold). Considering that 17β-estradiol treatment did not induce the SUMOylation of MTA1 (Fig. 8, *A* and *B*), it is reasonable to suggest that the increased recruitment of MTA1 or the MTA1·SUMO2/3 complex onto the *PS2* promoter upon 17β-estradiol treatment may be simply due to the increased recruitment of the NuRD complex.

Consistent with the notion that SUMO conjugation on Lys-509 together with SIM synergistically regulate the transcriptional repressive activity of MTA1, the binding of HDAC2 with MTA1 at *PS2* promoter may also involve this synergistic regulatory mechanism, for MTA1-K509R/AAA mutant exhibited the least HDAC2 binding at *PS2* promoter among all three mutants (Fig. 9*F*). The plausible explanation could be that SUMOylated Lys-509 and SIM may use different ways to interact with HDAC2. Because of the increased binding between SUMOylated MTA1 and HDAC2 observed when Lys-509 was conjugated by SUMO2 *in vitro* (Fig. 9, *G* and *H*), SUMO-conjugated Lys-509 may be involved in the direct binding with HDAC2. However, SIM may affect the interaction between SUMOylated MTA1 and HDAC2 through its ability to fine-tune the SUMOylation of MTA1. Alternatively, SIM may interact intramolecularly with the SUMO moiety conjugated to the lysine residue within the non-consensus site, resulting in the recruitment of HDAC2. The discovery that enhanced binding of SUMOylated MTA1 and HDAC2 was also detected *in vitro* when SUMOylation occurred on a non-consensus lysine residue (Fig. 9, *G* and H) supports the above two points. It is worth mentioning that although in this study we have discussed the involvement of HDAC2 in MTA1-mediated repression on *PS2* transcription, we cannot rule out the possibility that another co-repressor may participate in the regulating *PS2* transcription through SUMOylated Lys-509 and SUMO-SIM interaction, because the MTA1-AAA mutant showed less SUMO2/3 association but more HDAC2 binding at the *PS2* promoter compared with the MTA1-K509R mutant (Fig. 9*F*).

The reason why MTA1 harbors multiple potential SUMOylation sites is unclear. Possibly, some sites act as backup to prevent the loss of SUMOylation of MTA1, which may be important for its function. Alternatively, the interactions of the SIM and SUMO moieties at different lysine residues other than Lys-509 may produce different conformations, which could provide docking sites for different co-repressors. Binding with different partners is one way that MTA1 modulates gene transcription. The synergistic regulatory mechanism of SUMOylation and the SUMO-SIM interaction may provide MTA1 more options to spatially and temporally coordinate different co-regulators and subsequently participate in multiple signaling pathways.

MTA1 Up-regulates the Expression of SUMO2—Increasing studies have shown that SUMO homeostasis plays important roles in cancer progression (31). For example, elevated mRNA levels of SENP1 and SENP3 were detected in tissues from human prostate cancer patients (32, 33). In addition, the inoculation of MCF-7 cells overexpressing UBC9 as xenografts in mice revealed that tumors expressing UBC9 grew better than the vector control (34). The SUMOylation of reptin turns off the expression of *KAI1*, a metastasis suppressor gene, leading to the enhanced metastatic ability of cancer cells (35). Also, it is known that MTA1 is expressed ubiquitously and overproduced in breast, lung, gastric, colorectal, and pancreatic cancers (36). Overexpression of MTA1 in breast cancer cells significantly enhances the invasive ability of these cells to invade in an anchorage-independent manner by reducing the levels of ER target genes, including *PS2* (10). A recent study reports that a deficiency of *PS2* increases the tumorigenicity of human breast cancer cells and mammary tumor development in *PS2* knock-out mice (37). Therefore, our study of the expression of *SUMO2* being up-regulated by MTA1 provides a clue that MTA1 may contribute to the metastatic ability of cells by modulating the SUMOylation pathway, which in turn regulates the repressive effect of MTA1 on its target gene, *e.g. PS2*. Interestingly, neither SUMOylation of MTA1 nor the SUMO-SIM interaction is likely to be involved in modulating *SUMO2* transcription, as we could not detect the association of the MTA1·SUMO2/3 complex at the *SUMO2* promoter (supplemental Fig. S4), implying that the regulation of transcriptional activity of MTA1 by SUMO may depend on the promoter context.

In summary, our findings presented here not only suggest a synergistic regulatory mechanism of SUMO modification and SIM in MTA1-mediated transcription but also uncover a potential function of MTA1 in modulating the SUMOylation pathway. Further identification of SUMO-dependent novel target genes or co-factors of MTA1 would help us to better understand the function of MTA1 in human cancer.

Acknowledgments—We gratefully thank Drs. Mary Dasso, Jorma J. Palvimo, Frank J. Rauscher III, David J. Shapiro, Andrew D. Sharrocks, and Weidong Wang for generous gifts of expression plasmids. We also acknowledge all members of the Kumar laboratory for technical assistance and fruitful discussion, and especially, we are grateful to Prakriti Mudvari for data mining and Amanda J. Lyon for critical reading of this manuscript.

REFERENCES

1. Mahajan, R., Gerace, L., and Melchior, F. (1998) *J. Cell Biol.* **140,** 259–270
2. Klenk, C., Humrich, J., Quitterer, U., and Lohse, M. J. (2006) *J. Biol. Chem.* **281,** 8357–8364
3. Lin, D. Y., Huang, Y. S., Jeng, J. C., Kuo, H. Y., Chang, C. C., Chao, T. T., Ho, C. C., Chen, Y. C., Lin, T. P., Fang, H. I., Hung, C. C., Suen, C. S., Hwang, M. J., Chang, K. S., Maul, G. G., and Shih, H. M. (2006) *Mol. Cell* **24,** 341–354
4. Rytinki, M. M., Kaikkonen, S., Pehkonen, P., Jääskeläinen, T., and Palvimo, J. J. (2009) *Cell Mol. Life Sci.* **66,** 3029–3041
5. Gareau, J. R., and Lima, C. D. (2010) *Nat. Rev. Mol. Cell Biol.* **11,** 861–871
6. Kerscher, O. (2007) *EMBO Rep.* **8,** 550–555
7. Saether, T., Pattabiraman, D. R., Alm-Kristiansen, A. H., Vogt-Kielland, L. T., Gonda, T. J., and Gabrielsen, O. S. (2011) *Oncogene* **30,** 212–222
8. Meulmeester, E., Kunze, M., Hsiao, H. H., Urlaub, H., and Melchior, F. (2008) *Mol. Cell* **30,** 610–619
9. Toh, Y., Oki, E., Oda, S., Tokunaga, E., Ohno, S., Maehara, Y., Nicolson, G. L., and Sugimachi, K. (1997) *Int. J. Cancer* **74,** 459–463
10. Mazumdar, A., Wang, R. A., Mishra, S. K., Adam, L., Bagheri-Yarmand, R., Mandal, M., Vadlamudi, R. K., and Kumar, R. (2001) *Nat. Cell Biol.* **3,** 30–37
11. Mishra, S. K., Mazumdar, A., Vadlamudi, R. K., Li, F., Wang, R. A., Yu, W., Jordan, V. C., Santen, R. J., and Kumar, R. (2003) *J. Biol. Chem.* **278,** 19209–19219
12. Gururaj, A. E., Singh, R. R., Rayala, S. K., Holm, C., den Hollander, P., Zhang, H., Balasenthil, S., Talukder, A. H., Landberg, G., and Kumar, R. (2006) *Proc. Natl. Acad. Sci. U.S.A.* **103,** 6670–6675
13. Li, D. Q., Ohshiro, K., Reddy, S. D., Pakala, S. B., Lee, M. H., Zhang, Y., Rayala, S. K., and Kumar, R. (2009) *Proc. Natl. Acad. Sci. U.S.A.* **106,** 17493–17498
14. Ohshiro, K., Rayala, S. K., Wigerup, C., Pakala, S. B., Natha, R. S., Gururaj, A. E., Molli, P. R., Månsson, S. S., Ramezani, A., Hawley, R. G., Landberg, G., Lee, N. H., and Kumar, R. (2010) *EMBO Rep.* **11,** 691–697
15. Talukder, A. H., Mishra, S. K., Mandal, M., Balasenthil, S., Mehta, S., Sahin, A. A., Barnes, C. J., and Kumar, R. (2003) *J. Biol. Chem.* **278,** 11676–11685
16. Kane, S., Sano, H., Liu, S. C., Asara, J. M., Lane, W. S., Garner, C. C., and Lienhard, G. E. (2002) *J. Biol. Chem.* **277,** 22115–22118
17. Tatham, M. H., Rodriguez, M. S., Xirodimas, D. P., and Hay, R. T. (2009) *Nat. Protoc.* **4,** 1363–1371
18. Stankovic-Valentin, N., Deltour, S., Seeler, J., Pinte, S., Vergoten, G., Guérardel, C., Dejean, A., and Leprince, D. (2007) *Mol. Cell. Biol.* **27,** 2661–2675
19. Pichler, A., Gast, A., Seeler, J. S., Dejean, A., and Melchior, F. (2002) *Cell* **108,** 109–120
20. Minty, A., Dumont, X., Kaghad, M., and Caput, D. (2000) *J. Biol. Chem.* **275,** 36316–36323
21. Song, J., Durrin, L. K., Wilkinson, T. A., Krontiris, T. G., and Chen, Y. (2004) *Proc. Natl. Acad. Sci. U.S.A.* **101,** 14373–14378
22. Hannich, J. T., Lewis, A., Kroetz, M. B., Li, S. J., Heide, H., Emili, A., and Hochstrasser, M. (2005) *J. Biol. Chem.* **280,** 4102–4110
23. Knipscheer, P., Flotho, A., Klug, H., Olsen, J. V., van Dijk, W. J., Fish, A., Johnson, E. S., Mann, M., Sixma, T. K., and Pichler, A. (2008) *Mol. Cell* **31,** 371–382
24. Zhu, J., Zhu, S., Guzzo, C. M., Ellis, N. A., Sung, K. S., Choi, C. Y., and Matunis, M. J. (2008) *J. Biol. Chem.* **283,** 29405–29415
25. Rosendorff, A., Sakakibara, S., Lu, S., Kieff, E., Xuan, Y., DiBacco, A., Shi, Y., Shi, Y., and Gill, G. (2006) *Proc. Natl. Acad. Sci. U.S.A.* **103,** 5308–5313
26. Wu, H., Sun, L., Zhang, Y., Chen, Y., Shi, B., Li, R., Wang, Y., Liang, J., Fan, D., Wu, G., Wang, D., Li, S., and Shang, Y. (2006) *J. Biol. Chem.* **281,** 21848–21856
27. Sentis, S., Le Romancer, M., Bianchin, C., Rostan, M. C., and Corbo, L. (2005) *Mol. Endocrinol.* **19,** 2671–2684
28. Métivier, R., Penot, G., Hübner, M. R., Reid, G., Brand, H., Kos, M., and Gannon, F. (2003) *Cell* **115,** 751–763
29. Zhu, S., Goeres, J., Sixt, K. M., Békés, M., Zhang, X. D., Salvesen, G. S., and Matunis, M. J. (2009) *Mol. Cell* **33,** 570–580
30. Pichler, A., Knipscheer, P., Saitoh, H., Sixma, T. K., and Melchior, F. (2004) *Nat. Struct. Mol. Biol.* **11,** 984–991
31. Bawa-Khalfe, T., and Yeh, E. T. (2010) *Genes Cancer* **1,** 748–752
32. Cheng, J., Bawa, T., Lee, P., Gong, L., and Yeh, E. T. (2006) *Neoplasia* **8,** 667–676
33. Han, Y., Huang, C., Sun, X., Xiang, B., Wang, M., Yeh, E. T., Chen, Y., Li, H., Shi, G., Cang, H., Sun, Y., Wang, J., Wang, W., Gao, F., and Yi, J. (2010) *J. Biol. Chem.* **285,** 12906–12915
34. Mo, Y. Y., Yu, Y., Theodosiou, E., Ee, P. L., and Beck, W. T. (2005) *Oncogene* **24,** 2677–2683
35. Kim, J. H., Choi, H. J., Kim, B., Kim, M. H., Lee, J. M., Kim, I. S., Lee, M. H., Choi, S. J., Kim, K. I., Kim, S. I., Chung, C. H., and Baek, S. H. (2006) *Nat. Cell Biol.* **8,** 631–639
36. Nicolson, G. L., Nawa, A., Toh, Y., Taniguchi, S., Nishimori, K., and Moustafa, A. (2003) *Clin. Exp. Metastasis* **20,** 19–24
37. Buache, E., Etique, N., Alpy, F., Stoll, I., Muckensturm, M., Reina-San-Martin, B., Chenard, M. P., Tomasetto, C., and Rio, M. C. (2011) *Oncogene* **30,** 3261–3273